

Boolean matrix logic programming for active learning of gene functions in genome-scale metabolic network models

Lun Ai · Stephen H. Muggleton · Shi-Shun Liang · Geoff S. Baldwin

Abstract Techniques to autonomously drive research have been prominent in Computational Scientific Discovery, while Synthetic Biology is a field of science that focuses on designing and constructing new biological systems for useful purposes. Here we seek to apply logic-based machine learning techniques to facilitate cellular engineering and drive biological discovery. Comprehensive databases of metabolic processes called genome-scale metabolic network models (GEMs) are often used to evaluate cellular engineering strategies to optimise target compound production. However, predicted host behaviours are not always correctly described by GEMs, often due to errors in the models. The task of learning the intricate genetic interactions within GEMs presents computational and empirical challenges. To address these, we describe a novel approach called Boolean Matrix Logic Programming (BMLP) by leveraging boolean matrices to evaluate large logic programs. We introduce a new system, *BMLP_{active}*, which efficiently explores the genomic hypothesis space by guiding informative experimentation through active learning. In contrast to sub-symbolic methods, *BMLP_{active}* encodes a state-of-the-art GEM of a widely accepted bacterial host in an interpretable and logical representation using datalog logic programs. Notably, *BMLP_{active}* can successfully learn the interaction between a gene pair with fewer training examples than random experimentation, overcoming the increase in experimental design space. *BMLP_{active}* enables rapid optimisation of metabolic models to reliably engineer biological systems for producing useful compounds. It offers a realistic approach to creating a self-driving lab for microbial engineering.

Keywords Computational Scientific Discovery; Synthetic Biology; Active Learning; Inductive Logic Programming; Matrix.

Lun Ai (corresponding author)
Department of Computing, Imperial College London, London, UK
E-mail: lun.ai15@imperial.ac.uk

Stephen H. Muggleton
Department of Computing, Imperial College London, London, UK
E-mail: s.muggleton@imperial.ac.uk

Shi-Shun Liang
Department of Life Sciences, Imperial College London, London, UK
E-mail: shishun.liang20@imperial.ac.uk

Geoff S. Baldwin
Department of Life Sciences, Imperial College London, London, UK
E-mail: g.baldwin@imperial.ac.uk

1 Introduction

A priority in scientific research is the development of autonomous systems to enhance the scientific discovery process. Currently, most efforts in this domain focus on either laboratory automation or machine learning applied to scientific datasets. Sub-symbolic approaches usually demand a large number of annotated data and extensive trial-and-error. It is often difficult to modify the structure of these machine learning systems or extract human-interpretable information. The application of these systems in an experimental workflow is limited by data efficiency, flexibility and interpretability. There is a resurgence of interest in incorporating AI in experimental automation and scientific understanding simultaneously. In this work, we investigate an integration of techniques for planning experiments, optimising resource utilisation and interpretable machine learning to support biological discovery.

In the pursuit of understanding natural phenomena, scientists often formulate plausible theories and design experiments to test competing hypotheses. This process typically involves a careful selection of experimental conditions and the logical inference mechanism of abduction. Experimentation can be optimised through active learning, where computational methods are employed to strategically select informative training examples to combat resource limitations. On the other hand, Inductive Logic Programming (ILP) [49] offers an automated approach to abduction, representing observations, hypotheses and background knowledge through interpretable logic programs. In ILP, hypotheses are learned to explain observational data with respect to the background knowledge. “Askable” hypotheses, known as abducibles, that might explain contradictions between observations and known background knowledge are first assumed to hold [14]. The resulting extended knowledge, enriched with abducted hypotheses, is subsequently verified against observations [52].

Our study explores the applicability of abductive reasoning and active learning to comprehensive biological systems. Given that biological relationships are commonly described logically, ILP is particularly adept at operating on biological knowledge bases. The integration of abductive reasoning and active learning via ILP was successfully demonstrated in the context of biological discovery by the prominent Robot Scientist [39]. The Robot Scientist performed active learning by strategically selecting key experiments to achieve more data- and cost-effective gene function learning than random experimentation. However, this demonstration was limited to only 17 genes in the aromatic amino acid pathway of yeast. In the present study, we advance the scope of logic-based gene function learning by looking at *Escherichia coli* (*E. coli*). The genome-scale metabolic model (GEM), iML1515 [48], encompasses 1515 genes and 2719 metabolic reactions of the *E. coli* strain K-12 MG1655, a versatile host organism for metabolic engineering to produce specific compounds. Notably, the iML1515 model represents a 90-fold increase in complexity compared to the aromatic amino acid pathway investigated by the Robot Scientist.

Despite the extensive mapping of the *E. coli* genome to metabolic functions in iML1515, it was shown to yield inaccurate phenotype predictions [9]. A classical method to address errors in metabolic pathways involves auxotrophic growth experiments, where specific genes are deleted to render the organism incapable of synthesizing essential compounds [6]. For accurate simulation of auxotrophic mutant experiments, the computational representation of GEMs must faithfully depict the underlying network structure and effectively facilitate the exploration of metabolic pathways.

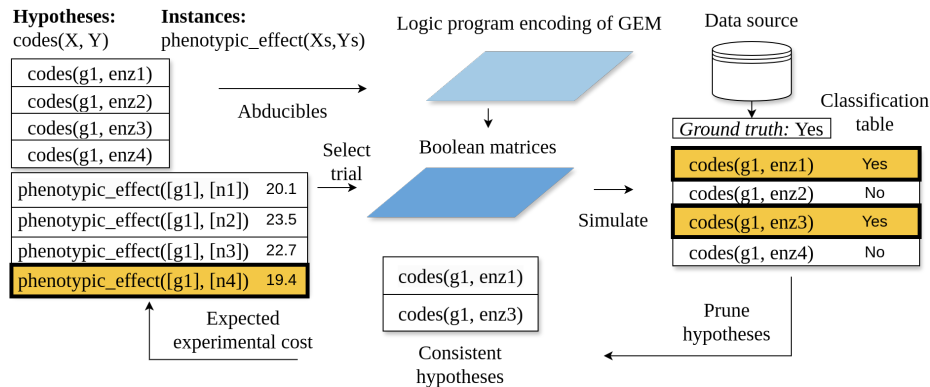


Fig. 1: The hypotheses and instances are represented as logic programs to describe gene functions (gene-enzyme associations) and auxotrophic mutant experiment conditions respectively. *BMLP_{active}* encodes the GEM iML1515 and simulates the auxotrophic mutant experiment outcomes. It actively consults a data source to request ground truth labels that minimise the expected experimental cost based on a user-provided cost function when pruning hypotheses. The underlying BMLP iteratively refutes gene function hypotheses inconsistent with labelled training examples. While *BMLP_{active}* to date only learns from synthetic data, a laboratory robot can be integrated to perform selected experiments.

Considering these requirements, Petri nets emerge as suitable modelling tools for GEMs. Petri nets are a class of directed bipartite graphs with diverse applications in Computer Science and Biology [61, 64]. Petri nets can represent a structured knowledge base while capturing dynamic behaviours in a system. In contrast, logic programs allow reasoning over relationships between entities but cannot directly reflect the changes in concepts and entity states. To integrate logic reasoning with Petri nets, we explore a more holistic approach to learning metabolic networks that combines recursive logic programs with pathway reachability analysis.

Learning complex biological systems like GEMs presents significant challenges in terms of computational complexity and empirical feasibility. To address these challenges, we present a new system *BMLP_{active}* (Figure 1) based on a novel approach called Boolean Matrix Logic Programming (BMLP) and an implementation in SWI-Prolog. We use logic programs to encode the biochemical, genetic, and genomic relationships in iML1515. While simulating auxotrophic mutant experiments, logical inferences to predict phenotypic effects are accelerated by boolean matrices via BMLP. This speeds up the runtime for predicting phenotypic effects by a factor of 170 compared to SWI-Prolog without BMLP on a single computation thread. We implement active learning to select auxotrophic mutant experiments that minimise the expected experimental cost via a user-defined cost function. Empirically, we delete gene functions in iML1515 and use *BMLP_{active}* to learn hypotheses to recover the deleted gene functions. *BMLP_{active}* successfully restores these removed gene functions through active learning while reducing 90% the optional nutrient substance cost required by randomly selected experiments. It additionally lowers the number of experimental data needed to recover these gene functions compared to random ex-

periment selection, reducing the sample complexity. When operating within a finite budget, our approach can deliver optimal experimental outcomes, whereas studies employing random experiment selection might not reach completion.

Furthermore, we apply $BMLP_{active}$ to learning digenic functions, which holds significant implications for drug development and therapeutic interventions [22]. These digenic interactions are related to isoenzymes - two enzymes responsible for the same reaction. The intricate relationship between complex genotypes and phenotypes remains largely unexplored in most organisms [21]. Additionally, some digenic interactions are dynamic and can vary depending on the growth conditions [9]. A comprehensive understanding of digenic interactions would expedite strain engineering efforts. We show that $BMLP_{active}$ can converge to the correct gene-isoenzyme mapping with as little as 20 training examples. This shows a significant promise for $BMLP_{active}$ to address complex genetic interactions on the whole genome level.

Our contributions are:

1. We describe a novel problem of Boolean Matrix Logic Programming (BMLP).
2. We implement a BMLP algorithm, BMLP-IE, in SWI-Prolog to predict phenotypic effects by computing reachability queries in GEMs based on a subclass of Petri net, which empirically improves simulation runtime by 170-fold compared to SWI-Prolog without BMLP-IE.
3. We built a BMLP system, $BMLP_{active}$, which uses BMLP-IE to actively select experiment instances for learning gene functions in a GEM.
4. We present a theoretical sample complexity ratio between active learning and random experiment sampling and empirically highlight the effect of actively selecting examples in reducing the total training examples needed.
5. We empirically show that $BMLP_{active}$ reduces 90% optional nutrient substance cost and the number of experiments needed for learning gene functions compared to randomly sampled experiments.
6. Our empirical results demonstrate that $BMLP_{active}$ can be devised to learn gene-isoenzyme associations in GEM with a faster convergence to the correct gene-isoenzyme mapping than randomly sampled experiments.

The rest of this paper is organised as follows. In Section 2, we summarise work on machine learning of genome-scale metabolic networks, matrix algebra, Petri nets and active learning. In Section 3, we introduce key concepts in matrix algebra and an elementary class of Petri nets that we use to model a GEM, called one-bounded elementary nets (OENs). In Section 4, we describe a transformation from an OEN to a subclass of recursive logic programs, linear and immediately recursive datalog. In Section 5, we introduce our BMLP framework to evaluate this class of logic programs. In Section 6, we describe our active learning approach based on prior work [14, 50]. In Section 7, we explain the $BMLP_{active}$ implementation for encoding iML1515, GEM simulation and active learning gene functions. Section 8 includes our empirical results on simulation runtime, phenotype prediction, active learning gene functions and gene-isoenzyme mapping. In Section 9, we explain the current limitations of $BMLP_{active}$ and discuss future work.

2 Related work

2.1 Active learning in computational scientific discovery

Active learning techniques provide machine learning algorithms with more control over the training examples they use [18]. A typical approach to active learning is via membership queries where the machine learner queries a data source to label instances according to some strategy. An active learner can be implemented to explore the version space which contains all hypotheses that are expressible by a hypothesis language and are consistent with a set of training examples [47]. Instances are chosen according to a measure of informativeness such as entropy [71], diameter [76], the size [47,25] and the shrinkage [36] of the version space for eliminating competing hypotheses. For a binary classification task, when learners are allowed to look at n unlabelled instances to compare, an active learner has n times larger probability of selecting an instance with maximal entropy than a passive learner [36]. The general principle for a binary active learner is to label instances closest to being consistent with half of the hypotheses in the version space [47]. These instances reject up to half of the hypothesis space regardless of their classifications. In the optimal case when all instances are maximally discriminative, the target hypothesis can be found via a binary search with depth logarithmic of the hypothesis space size [4]. *BMLP_{active}* makes membership queries but our objective is to not only reduce the number of labels but also minimise the expected cost of experimentation.

Computational systems such as the BACON systems [42], the LAGRANGE systems [75], recent equation discovery systems [13,34,58] are primarily designed to formulate symbolic hypotheses from experimental results. However, one cannot directly employ these systems for experimental planning. The automation of experimental design was investigated by the pioneering Robot Scientist [39] as an endeavour to bring together logical reasoning, active learning and laboratory automation. The Robot Scientist automatically proposes explanatory hypotheses, actively devises validation experiments, performs experiments using laboratory robotics, and interprets empirical observations. Abduction and active learning are supported by ASE-Progol [14] based on the ILP system Progol [50]. Experiments were actively selected to minimise the expected cost of experimentation for learning gene functions in the aromatic amino acid synthesis pathway of yeast. It was combined with a laboratory robot to automatically reconstruct the yeast metabolic pathway model and the active learning strategy significantly outperformed random experiment selection [39]. Later, a high-throughput laboratory automation platform, Adam [38] extended this approach by constructing a logical model of yeast consisting of 1200 genes. In comparison, we apply *BMLP_{active}* to a genome-scale metabolic network, which is significantly larger than the models in [39,38].

Recently, large language models (LLMs) have been explored to automate experimental design via user-provided prompt texts [11,12]. LLMs are generative models of natural languages based on neural networks that are trained from textual data. In [11,12], LLMs served as experiment planners and coding assistants. These platforms use LLMs for planning experimental steps using publicly available knowledge bases, writing and interpretation programs to control hardware in a laboratory environment and analysing collected experimental data. Their advantage is accessing rich information online and interacting with users while designing experiments. However, the consistency and faithfulness of their outputs cannot be guaranteed. It has been

stressed that autonomous experimentation by AI should be employed with caution without the means to identify the source of error and explain observations [62]. While $BMLP_{active}$ cannot yet interact with biologists in natural language, interpreting and verifying its output are straightforward due to its logical representation and computation.

2.2 Learning genome-scale metabolic network models

GEMs contain known metabolic reactions in organisms, serving as functional knowledge bases for their metabolic processes. There has been an increasing interest in integrating machine learning methods with GEMs to improve the predictions of gene-phenotype correlations within biological systems [3,70]. This often requires constraint-based modelling techniques for simulating GEMs [60]. Flux balance analysis (FBA) [56] is the most common mathematical approach to solve flux distributions in genome-scale models under the steady-state condition. FBA uses linear programming to model fluxes in a chemical reaction network represented by a matrix that contains the stoichiometric coefficients of metabolites in reactions. Ensemble learning frameworks such as [79,55,35] obtain support vector machines, decision trees and artificial neural networks to represent hidden constraints between genetic factors and metabolic fluxes. These systems cannot identify inconsistencies between simulation results and experimental data to self-initialise constraints to aid learning [60]. On the other hand, mechanistic information that reflects whole-cell dynamics has been incorporated to address these concerns, for instance in artificial neural networks to tune their parameters [81]. The hybrid approach in [30] embeds FBA within artificial neural networks based on custom loss functions surrogating the FBA constraints. Recent research also explores autoencoders for learning the underlying relationship between gene expression data and metabolic fluxes via fluxes estimated by FBA [64]. Currently, machine learning of genome-scale metabolic networks is significantly limited by the availability of training data [70]. In contrast, $BMLP_{active}$ does not use FBA so it is not dependent on the metabolic flux constraints. $BMLP_{active}$ also performs active learning to reduce the cost and the number of experiments. This is a notable advantage considering finite experiment resources and insufficient experimental data.

2.3 Matrix algebraic approaches to logic programming

In our BMLP framework, we use boolean matrices to evaluate fixpoints of large recursive datalog programs. Obtaining the least Herbrand model of recursive datalog programs can be reduced to computing the transitive closure of boolean matrices [57,20]. Fischer and Meyer [31] study a divide-and-conquer boolean matrix computation technique by viewing relational databases as graphs. A similar approach is explored by Ioannidis [37] for computing the fixpoint of recursive Horn clauses. An ILP system called DeepLog [51] employs boolean matrices for learning recursive datalog programs. It repeatedly computes square boolean matrices to quickly choose optimal background knowledge for deriving target hypotheses. The mapping from biological knowledge bases to propositional logic programs is explored in [69,67] where logic programs are represented as boolean matrices by considering gene

regulatory networks as boolean networks. In contrast, we encode a GEM as a Petri net and a recursive datalog program for computing reachability queries.

Recent work primarily studies the mapping of logic programs to linear equations over tensor spaces. SAT problems are investigated in [43] under a linear algebra framework. Truth values of domain entities, logical relations and operators for first-order logic can be evaluated using tensors-based calculus [33]. Computing algebraic solutions can approximate recursive relations in first-order Datalog [66]. Based on this approach, abduction can be performed by encoding a subset of recursive datalog programs in tensor space [68]. Tensor representations allow differentiable infrastructures such as neural networks to perform probabilistic logical inferences [17]. This can be done using dynamic programming to propagate beliefs for stochastic first-order logic programs. The probabilistic parameters can be optimised using deep learning frameworks [80]. Limitations have been identified for solving certain recursive programs due to the difficulty of computing some arithmetic solutions whereas these can be solved by iterative bottom-up evaluations [66]. In addition, algebraic approximations are usually calculated in linear algebraic methods where the correctness of the solutions cannot be guaranteed. However, our BMLP approach does not have these issues since it uses boolean matrices for iterative bottom-up computation.

2.4 Petri nets in logic programming

Little attention has been paid to representing and simulating Petri nets with logic programs. With logic programming, techniques to execute, analyse and learn Petri nets can be implemented in a single programming language [28]. The early work [28] describes places and transitions of a Petri net in terms of n-ary ground facts. Srinivasan et al. [73] attempt to learn n-ary ground facts that represent Petri net transitions in the ILP [49] system Aleph [72]. Few studies have looked at encoding Petri nets by Answer Set Programming (ASP) [32]. Behrens and Dix [7] use Petri nets for analysing interactions in multi-agent systems with ASP programs. Anwar et al. [5] provide an ASP encoding of Petri nets with coloured tokens to model the behaviours of biological systems. This encoding is adapted by Dimopoulos et al. [27] for simulating reversible Petri nets that allow transitions to fire in both directions. These systems all use high-level symbolic representations of Petri nets as deductive knowledge bases. Logic programming approaches rely on navigating background knowledge to determine the consistency of hypotheses. However, non-high-throughput deductive inferences limit these systems' applicability for dealing with increasingly complex knowledge bases such as GEMs. *BMLP_{active}* addresses this limitation by utilising a boolean matrix encoding of GEMs and boolean matrix operations to accelerate inferences.

3 Preliminaries

3.1 Matrix algebra for datalog

We introduce datalog programs and concepts relating to our BMLP framework based on [44, 54]. A variable is a character string beginning with an uppercase letter. A function, predicate or constant symbol is a character string starting with a lowercase

letter. A term is either a variable, a constant symbol, or a function symbol attached to a tuple of terms. A ground term contains no variables. An atom is a predicate symbol applied to a tuple of terms e.g. $r(a, Y)$ where r is a predicate symbol, a is a constant symbol and Y is a variable. An atom is ground when it contains only ground terms. A Horn clause is a disjunctive clause with at most one positive literal. A definite clause is a Horn clause with exactly one positive literal and a definite program is a set of definite clauses. A query is a user-posted Horn clause without any positive literal. A general logic program engine such as a Prolog interpreter can evaluate a query by carrying out a refutation proof of its negation via SLD resolutions (Selective Linear Definite clause resolution). A unit ground clause (fact) is a definite clause with no body literal and no variables. Datalog programs are definite programs without function symbols. A first-order definite clause has the form, $A_0 \leftarrow A_1, \dots, A_n$ where $A_i = r_i(x_1, \dots, x_k)$, r_i is a predicate symbol, x_j is a term. The arity of a function or predicate symbol is its number of arguments, e.g. r_i/k indicates r_i has arity k . The literal A_0 is called the head of the clause and the literals A_i are the body.

The Herbrand base $\mathcal{B}_{\mathcal{P}}$ is the set of all unit ground clauses provable from the predicate and constant symbols in a first-order definite program \mathcal{P} . The Immediate Consequence Operator $\mathcal{T}_{\mathcal{P}}$ [77] is a mapping over subsets of $\mathcal{B}_{\mathcal{P}}$ defined as:

$$\forall I \subseteq \mathcal{B}_{\mathcal{P}}, \mathcal{T}_{\mathcal{P}}(I) = \{\alpha \in \mathcal{B}_{\mathcal{P}} \mid \alpha \leftarrow B_1, \dots, B_m \ (m \geq 0) \\ \text{is a ground instance of a clause in } \mathcal{P} \text{ and } \{B_1, \dots, B_m\} \subseteq I\}.$$

$\mathcal{T}_{\mathcal{P}}$'s least fixpoint is $\mathcal{T}_{\mathcal{P}} \uparrow^{\omega} = \cup_{n \geq 0} \mathcal{T}_{\mathcal{P}} \uparrow^n$ where $\mathcal{T}_{\mathcal{P}} \uparrow^0 = \emptyset$ and $\mathcal{T}_{\mathcal{P}} \uparrow^n = \mathcal{T}_{\mathcal{P}}(\mathcal{T}_{\mathcal{P}} \uparrow^{n-1})$. A clause entailed by \mathcal{P} is written as $\mathcal{P} \models \alpha$. The minimal Herbrand model $M(\mathcal{P})$ contains all unit ground clauses that are entailed by \mathcal{P} and $M(\mathcal{P}) = \mathcal{T}_{\mathcal{P}} \uparrow^{\omega}$.

A recursive program has a body literal that appears in the head of a clause. Specifically, we focus on linear and immediately recursive datalog as simple recursive datalog programs. A linear and immediately recursive datalog program has a single recursive clause with the recursive predicate appearing in the body only once [37]. This subset of recursive datalog programs can represent the relational structure of reaction pathways. This is further elaborated in Section 4. An example of a linear and immediately recursive datalog program involving one non-recursive predicate is:

$$r_2(X, Y) \leftarrow r_1(X, Y). \\ r_2(X, Y) \leftarrow r_1(X, Z), r_2(Z, Y).$$

A recursive datalog program \mathcal{P} can be written as matrices for bottom-up evaluation [15]. When \mathcal{P} is linear and immediately recursive, it can be described by linear equations [66]:

$$\mathbf{R}_2^0 = \mathbf{0} \\ \mathbf{R}_2^k = \mathbf{R}_1 + \mathbf{R}_1 \mathbf{R}_2^{k-1}$$

where unit ground clauses r_1 and a recursive clause r_2 can be represented as matrices $\mathbf{R}_1, \mathbf{R}_2$ such that $(\mathbf{R}_k)_{i,j} = 1$ if $\mathcal{P} \models r_k(c_i, c_j)$ for constant symbols c_i, c_j and $(\mathbf{R}_k)_{i,j} = 0$ otherwise. Addition “+” between two boolean matrices is defined as $(\mathbf{A} + \mathbf{B})_{i,j} = \mathbf{A}_{i,j} \vee \mathbf{B}_{i,j}$. Multiplication “ \times ” is defined as $(\mathbf{A} \times \mathbf{B})_{i,j} = \bigvee_{k=1}^n \mathbf{A}_{i,k} \wedge \mathbf{B}_{k,j}$ and is abbreviated as \mathbf{AB} .

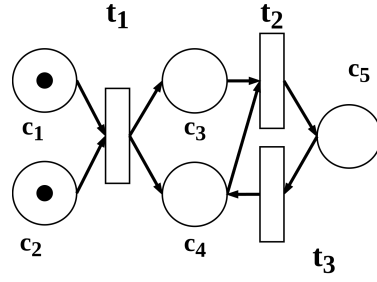


Fig. 2: A one-bounded elementary net (OEN). Places are ellipses. Transitions are rectangles. Arcs are marked with weights. A black dot is a token. The initial marking is $m(c_1) = m(c_2) = 1$. Firing transition t_1 gives a new marking $\{c_3, c_4\}$.

3.2 Elementary nets

Petri nets have wide applications in Computer Science [61]. Elementary nets [63] are a class of Petri nets. We summarise key concepts and notions of Petri net and elementary nets from [61, 63]. A Petri net contains two disjoint sets of nodes: places P and transitions T . The flow relation $F \subseteq (P \times T) \cup (T \times P)$ describes arcs between nodes. All places can be marked by tokens which symbolise the resources distributed in the network. The assignment of tokens to places is called a marking (of tokens). For a transition t , the pre-set $\bullet t = \{p \in P \mid pFt\}$ contains places whose tokens would be consumed by t and its post-set $t\bullet = \{p \in P \mid tFp\}$ contains places that would receive tokens from t . Markings represent the states of a Petri net. The weight of an arc (p, t) or (t, p) is conventionally written as \overline{pt} or \overline{tp} . Elementary nets are basic Petri nets where transitions consume one token from the pre-set and relocate a token to the post-set. In an elementary net, an arc weight $\overline{pt} = 1$ if $(p, t) \in F$ and $\overline{tp} = 1$ if $(t, p) \in F$. An elementary net is a tuple (P, T, F) .

A one-bounded elementary net (OEN) is a class of elementary nets that has places marked with at most one token [61]. A marking m in OEN is a characteristic function $m : P \rightarrow \{0, 1\}$ defined as:

$$m(x) = \begin{cases} 1 & \text{if a token is assigned to } x \\ 0 & \text{otherwise} \end{cases}$$

A place p is marked if $m(p) = 1$. An initial marking corresponds to the initial state of an elementary net and its tokens. Figure 2 shows an example of OEN with an initial marking of tokens. A transition t is enabled by m if and only if for all arcs $(p, t) \in F$, $m(p) = 1$. A step $m \xrightarrow{t} m'$ is a fired transition resulting in a new marking according to:

$$m'(p) = \begin{cases} m(p) - 1 & \text{if } (p, t) \in F \\ m(p) + 1 & \text{if } (t, p) \in F \\ m(p) & \text{otherwise} \end{cases} \quad (1)$$

A marking m' is reachable from a marking m if and only a finite step sequence exists. A place is reachable from m if and only if m' is a reachable marking from m and $m'(p) = 1$. A marking can be written as a row vector $[1, 0, 1, \dots]$ where each element

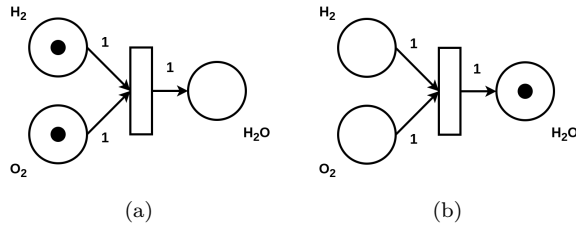


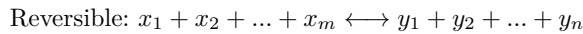
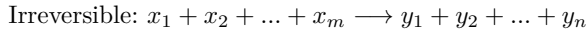
Fig. 3: OENs representing the qualitative relationship “ H_2 and O_2 produce H_2O ”. (a) Each place has up to one token. Each token represents the abundance of a chemical and this marking means H_2 and O_2 are available. (b) This model qualitatively describes that if H_2 and O_2 are available, then H_2O becomes available by firing the transition.

indicates if the respective place has a token. A transition can also be represented by a row vector $[z_1, z_2, \dots, z_k]$ where z_i reflects the assignment of tokens at the pre-set and post-set places. The consecutive firings of transition update markings and the global state of the system. This represents the dynamic changes in the distribution of tokenised resources.

4 Representing a GEM as a datalog program

4.1 Modelling a GEM with an OEN

We discuss the relationship between GEMs and OENs. Petri nets are commonly used formalism for representing complex biological systems such as genome-scale metabolic network models and diagnosing their dynamic behaviours [64]. A genome-scale metabolic network model contains biochemical reactions of substances. Reactants are substances initially involved in a reaction and the products are the chemicals yielded by a reaction. A reaction is reversible when the conversion of reactants to products and products to reactants can take place simultaneously. Reversible reactions are commonly treated as two reactions in opposite directions. A reaction involves chemical substances x_i and y_j :



A GEM is an OEN in the sense that a reaction is a transition, and reactants and products are places. Figure 3 presents a basic OEN modelling the water synthesis reaction involving H_2 , O_2 and H_2O .

Given an auxotrophic mutant experiment, we model a GEM as an OEN to find the set of synthesisable substances by following the metabolic reaction pathways. This requires computing the necessary set of places for transitions to fire. Transitions need to be enumerated to examine if their necessary conditions can ever be met for them to fire. Every simulation of GEM involves a definition of the growth medium consisting of essential chemicals for cellular metabolism such as amino acids, inorganic salts and carbon sources. The definition of a growth medium serves as the

basis of metabolic processes and gives an initial marking of OEN. Reachable places extending this marking are additional synthesisable substances.

4.2 Transforming an OEN into datalog

Each auxotrophic mutant experiment is treated as a datalog query to find all reachable places based on an initial marking. We evaluate queries of OEN reachability by transforming the OEN into a linear and immediately recursive datalog program. A datalog program consisting of clauses with arity two can be considered a directed graph where edges joining nodes represent the relation between terms. However, the multiplicity of the involved entities in a relation cannot be expressed this way. Instead, places and transitions are represented as constant and predicate symbols. Each argument of our transformed datalog program is a concatenation of constant symbols, e.g. $h2_o2$. For our specific purpose, since all place nodes in the OEN are related to metabolites, every new concatenated constant symbol describes a set of metabolic substances.

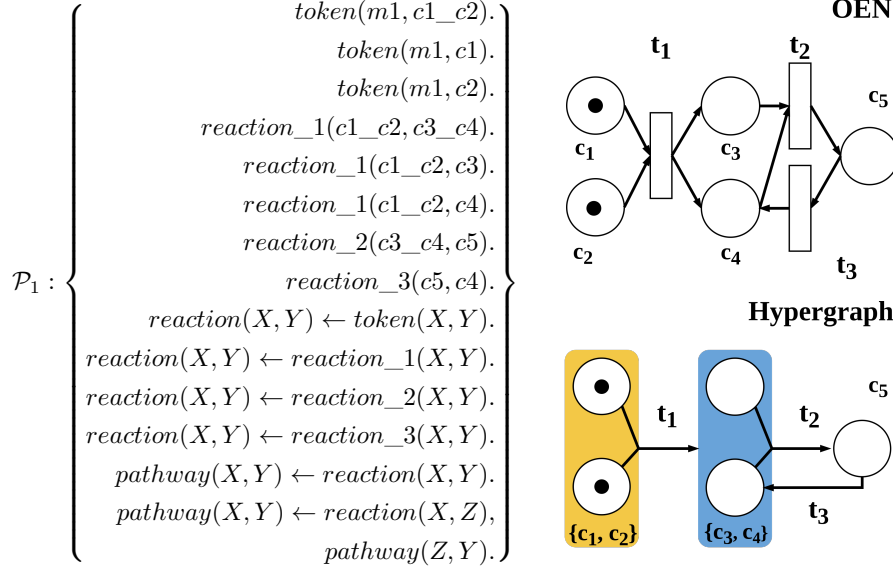
This transformation with constant symbol concatenation generalises from a directed graph into a hypergraph [8], a directed graph where an edge can connect to any number of nodes. Formally, a hypergraph $G = (V, E)$ is a tuple containing a set of nodes V and a set of edges $E \subseteq 2^V \times 2^V$ between arbitrary subsets of V . Hypernodes are sets of nodes connected by such edges. The incidence graph of a hypergraph is bipartite in that for $v \in V$ and $e \in E$, e is connected to v if and only if v and e are nodes connected by an edge in the bipartite graph. Given an OEN, we consider a hypergraph with an incidence graph of the same bipartite structure. A hypernode represents a set of place nodes and is created for every transition's input places from the OEN. Hypernodes are denoted by the new constant symbols that concatenate the member places' names, e.g. a hypernode $\{H_2, O_2\}$ is represented by the constant symbol $h2_o2$. The number of hypernodes we create is fixed and limited by the number of transitions. This is because each reaction has a finite number of reactants and products. The dynamic behaviour of an OEN is specified via an initial marking. This mapping between an OEN and a hypergraph allows us to write a datalog program. A recursive clause is added which describes a path in the hypergraph.

Definition 1 (OEN transformation) The transformation takes an OEN and an initial marking m . Let t denote any transition. Input places of transitions are represented by hypernodes p^* . A datalog program \mathcal{P} is written with predicate symbols t , r_1 and r_2 and variables X , Y and Z :

- write $token(m, p^*)$ if the marking m includes all members of a hypernode p^*
- write $token(m, q)$ if the marking m includes a place q
- write $t(p_1^*, p_2^*)$ if t connects two hypernodes p_1^* and p_2^*
- write $t(p^*, q)$ if t connects a hypernode p^* and a place q
- write $r_1(X, Y) \leftarrow token(X, Y)$ and $r_1(X, Y) \leftarrow t(X, Y)$ for every t clause written
- write $r_2(X, Y) \leftarrow r_1(X, Y)$ and $r_2(X, Y) \leftarrow r_1(X, Z), r_2(Z, Y)$

The transformed program is linear and immediately recursive since it contains only one recursive clause and the recursive predicate appears only once in the head of this clause. We illustrate how reachable places from an initial marking can be computed by evaluating the transformed program.

Example 1 Let the OEN in Figure 2 represent a metabolic pathway. Transitions t_1 , t_2 and t_3 are described by `reaction_1`, `reaction_2` and `reaction_3` clauses. We create two hypernodes denoted by `c1_c2` and `c3_c4`. These transitions connect places $\{c_3, c_4, c_5\}$ which are represented by constants $\{c_3, c_4, c_5\}$. For an initial marking $m_1 = \{c_1, c_2\}$, we can construct a datalog program \mathcal{P}_1 :



The right-hand-side figures are the OEN from Figure 2 and the hypergraph represented by \mathcal{P}_1 . The hypernode $\{c_3, c_4\}$ is reachable from $\{c_1, c_2\}$ via the transition t_1 . The place c_5 is reachable in two steps via transitions t_1 and t_2 . We can compute these by evaluating groundings of `pathway(m1, Y)` in the Herbrand model $M(\mathcal{P}_1)$ which gives us `pathway(m1, c2)`, `pathway(m1, c3_c4)` and `pathway(m1, c5)`.

We prove the correctness of computing reachable places in an OEN by evaluating the transformed datalog program. We first show the effect of a step (a fired transition) on updating markings. A step in an OEN updates the set of marked places.

Lemma 1 Let $OEN = (P, T, F)$. For a transition $t \in T$, marking m and m' , $\bigwedge_{p_i \in \bullet t} m(p_i) = 1 \rightarrow \bigwedge_{p_j \in t \bullet} m'(p_j) = 1$.

Proof It follows from Equation 1 that all tokens at the places in the pre-set of a transition are consumed and places in the post-set of a transition are assigned tokens.

Lemma 1 shows that when a transition t fires, in the new marking, tokens are re-assigned to other places. Given a marking, the set of marked places is a subset of P . The set of all token-to-place assignments is a power set $\Omega = 2^P$ and it is the union of all possible markings. From the property shown in Lemma 1, we define an operator called step consequence $\mathcal{T}_F : \Omega \rightarrow \Omega$.

Definition 2 (Step consequence operator \mathcal{T}_F) Given an OEN = (P, T, F), \mathcal{T}_F is an operator over the power set Ω :

$$\forall S \in \Omega, \mathcal{T}_F(S) = \{p_j \in P \mid p_j \in S' \leftarrow \wedge_{p_i \in \bullet t} p_i \in S\}$$

where $\{p_1, \dots, p_n\} \subseteq S$ and $p_j \in t^\bullet, S' \in \Omega$

Definition 3 says that the result of applying \mathcal{T}_F to a marking is a set of places reachable from it. $\mathcal{T}_F(\emptyset)$ only includes the initial marking due to the antecedent of the implication being false. To obtain the union of all places reachable from an empty marking, we can apply \mathcal{T}_F repeatedly to its results. The recursive application of \mathcal{T}_F can be defined as $\mathcal{T}_F \uparrow^0 = \emptyset$ and $\mathcal{T}_F \uparrow^n = \mathcal{T}_F(\mathcal{T}_F \uparrow^{n-1})$. This corresponds to a lattice.

Proposition 1 $(\mathcal{T}_F, \subseteq)$ is a complete lattice.

Proof The proof follows from Definition 2. $(\mathcal{T}_F, \subseteq)$ is a complete lattice since Ω is a set partially ordered by set inclusion \subseteq where \mathcal{T}_F is an operator over the power set Ω . The top element P is the union of elements in Ω and the bottom element \emptyset is the intersection of elements in Ω .

Let (P, T, F) be an arbitrary OEN. Using Proposition 1, we show \mathcal{T}_F over the lattice $(\mathcal{T}_F, \subseteq)$ has a fixpoint. We refer to Tarski's fixpoint theorem [74], which states a monotonic operator on a complete lattice has a least fixpoint. We prove that \mathcal{T}_F is a monotonic operator.

Lemma 2 \mathcal{T}_F is a monotonic operator over Ω . For all $S_1, S_2 \in \Omega$, if $S_1 \subseteq S_2$ then $\mathcal{T}_F(S_1) \subseteq \mathcal{T}_F(S_2)$.

Proof This follows from Definition 2. We will always extend a marking by adding places reachable from it. Places in the current marking are reachable and are retained after applying \mathcal{T}_F . Therefore, \mathcal{T}_F is a monotonic operator.

We show that the least fixpoint of \mathcal{T}_F is the union of reachable places by proving that \mathcal{T}_F is a compact operator.

Lemma 3 \mathcal{T}_F is a compact operator over Ω . For all $S_1 \in \Omega$, if $p \in \mathcal{T}_F(S_1)$ then $p \in \mathcal{T}_F(S_2)$ for a finite $S_2 \subseteq S_1$.

Proof Assume $p \in \mathcal{T}_F(S_1)$. From Definition 2 and the assumption, since \mathcal{T}_F performs a step, a transition t exists and S_1 must contain all pre-set places. Take places S_2 that contains S_1 . From Lemma 1, we know that firing t give $S' \subseteq \mathcal{T}_F(S_2)$ and $p \in S'$.

Proposition 2 The operator \mathcal{T}_F has a least fixpoint equal to $\mathcal{T}_F \uparrow^\alpha = \cup_{n \geq 0} \mathcal{T}_F \uparrow^n$.

Proof \mathcal{T}_F is a monotonic function. According to Tarski's fixpoint theorem [74], the function \mathcal{T}_F has a least fixpoint $\mathcal{T}_F \uparrow^\alpha$ for some $\alpha \geq 0$. Since \mathcal{T}_F is also a compact operator, if $p \in \mathcal{T}_F(\mathcal{T}_F \uparrow^\alpha)$ then $p \in \mathcal{T}_F(\mathcal{T}_F \uparrow^n)$ for some $n \geq 0$ and $\mathcal{T}_F \uparrow^n \subseteq \mathcal{T}_F \uparrow^\alpha$. The union of subsets of $\mathcal{T}_F \uparrow^\alpha$ is $\cup_{n \geq 0} \mathcal{T}_F \uparrow^n$, which covers every member of the least fixpoint. Therefore, $\mathcal{T}_F \uparrow^\alpha = \cup_{n \geq 0} \mathcal{T}_F \uparrow^n$.

Proposition 2 shows that when we repeatedly apply the step consequence operator to the empty set, the least fixpoint is the union of reachable places. This allows us to compute this least fixpoint by iteratively computing steps and expanding the set of reachable places. We then show the correctness of finding reachable places in an OEN via evaluating the transformed linear and immediately recursive program

Theorem 1 *Let \mathcal{P} be a datalog program transformed from an OEN. For constant symbols c_1, c_2 in \mathcal{P} , $\mathcal{P} \models r(c_1, c_2)$ if and only if c_2 is reachable from c_1 in the OEN given an initial marking m .*

Proof Prove the forward implication. Assume $\mathcal{P} \models r(c_1, c_2)$. Constant symbols c_1 and c_2 represent place nodes in the OEN. We know $r(c_1, c_2)$ is in the least model. Based on the definition of the Immediate Consequence Operator [77], $r(c_1, c_2) \leftarrow B_1, \dots, B_i$ ($i \geq 0$) is a clause in \mathcal{P} and $\{B_1, \dots, B_i\} \subseteq \mathcal{T}_{\mathcal{P}} \uparrow^\omega$. From Definition 1, we know that B_1, \dots, B_i are unit ground clauses describing the pre-sets and post-sets of transitions. There exists $n \geq 0$ such that $c_1 \in \mathcal{T}_F \uparrow^n$. Following the transitions B_1, \dots, B_i , we can apply the operator \mathcal{T}_F to $\mathcal{T}_F \uparrow^n$. From Definition 2 and proposition 2, we know $c_2 \in \mathcal{T}_F \uparrow^\alpha$ so a set of marked places $S \in \Omega$ must contain c_2 . Therefore, c_2 is reachable from c_1 given an initial marking m .

Now we prove the backward implication. Assume c_2 is reachable from c_1 in the OEN given an initial marking m . We know from Proposition 2 that $c_1, c_2 \in \mathcal{T}_F \uparrow^\alpha$. From Definition 2, there exists a finite sequence of steps $m \xrightarrow{t_1} m_1 \xrightarrow{t_2} \dots \xrightarrow{t_k} m'$ where $m(c_1) = m'(c_2) = 1$ and $k \geq 0$. From Definition 1, the transformed program \mathcal{P} contains these transitions as unit ground clauses $\{B_1, \dots, B_k\} \subseteq \mathcal{B}_{\mathcal{P}}$ and recursive clauses $r(X, Y) \leftarrow r_1(X, Y)$ and $r(X, Y) \leftarrow r_1(X, Z), r(Z, Y)$. There is a grounding of the recursive clauses such that $r(c_1, c_2) \leftarrow B_1, \dots, B_k$. By applying the $\mathcal{T}_{\mathcal{P}}$ operator, we know $\mathcal{P} \models r(c_1, c_2)$.

Theorem 1 says that a program transformed from an OEN is logically equivalent to the OEN based on the fixpoint semantics in Proposition 2 for evaluating OEN reachability queries. In the next section, we explain how we leverage boolean matrix operations to evaluate datalog transformed from OENs.

5 Boolean matrix logic programming

5.1 Problem setting

We propose the Boolean Matrix Logic Programming (BMLP) problem. In contrast to traditional logic program evaluation, BMLP uses boolean matrices to evaluate datalog programs.

Definition 3 (Boolean Matrix Logic Programming (BMLP) problem) Let \mathcal{P} be a datalog program containing a set of clauses with predicate symbol r . The goal of Boolean Matrix Logic Programming (BMLP) is to find a boolean matrix \mathbf{R} encoded by a datalog program such that $(\mathbf{R})_{i,j} = 1$ if $\mathcal{P} \models r(c_i, c_j)$ for constant symbols c_i, c_j and $(\mathbf{R})_{i,j} = 0$ otherwise.

We focus on linear and immediately recursive datalog programs with at most two body literals to simulate a GEM. Our goal is to implement BMLP algorithms that can compute boolean matrices for evaluating large logic programs representing GEMs.

5.1.1 Creating boolean matrices

From a datalog program \mathcal{P} , we define mappings between constant symbols and binary codes. Consider a ground term u that concatenates n constant symbols c_1, c_2, \dots, c_n . We can represent u using a n -bit binary code. When c_k is in u the k -th bit of the binary code is 1, otherwise, it is 0. For a linear and immediately recursive clause r that takes such terms as arguments, two boolean matrices \mathbf{R}_1 and \mathbf{R}_2 are defined by mapping unit ground clauses used by r to binary codes. The two matrices in logic program format have $\{v_1(1, b_1^1), v_1(2, b_1^2), \dots\}$ and $\{v_2(1, b_2^1), v_2(2, b_2^2), \dots\}$ as their rows where $v_1(i, b_1^i)$ and $v_2(i, b_2^i)$ are the i -th rows of the boolean matrices \mathbf{R}_1 and \mathbf{R}_2 . In v_1 and v_2 clauses, b_1^i and b_2^i are binary codes to represent constant symbols u_1 and u_2 as r 's first and second arguments. \mathbf{R}_1 and \mathbf{R}_2 are defined such that $v_1(i, b_1^i)$ and $v_2(i, b_2^i)$ hold only when $\mathcal{P} \models r(u_1, u_2)$.

Example 2 We show boolean matrices created from \mathcal{P}_1 in Example 1. Individual substances are represented by constant symbols $c1, c2$ and $c3$. Sets of chemical substances are denoted by additional concatenated constant symbols, $c1_c2, c3_c4$. On the right-hand side, we create two boolean matrices \mathbf{R}_1 and \mathbf{R}_2 from the reaction clauses in \mathcal{P}_1 . Since the first `reaction_1` clause also contains the constant symbols of the other `reaction_1` clauses, to avoid redundancy, only one binary code is created for these clauses in \mathbf{R}_1 and \mathbf{R}_2 .

$$\mathcal{P}_1 : \left\{ \begin{array}{l} \dots \\ \text{reaction_1}(c1_c2, c3_c4). \\ \text{reaction_1}(c1_c2, c3). \\ \text{reaction_1}(c1_c2, c4). \\ \text{reaction_2}(c3_c4, c5). \\ \text{reaction_3}(c5, c4). \\ \dots \\ \text{reaction}(X, Y) \leftarrow \text{reaction_1}(X, Y). \\ \text{reaction}(X, Y) \leftarrow \text{reaction_2}(X, Y). \\ \text{reaction}(X, Y) \leftarrow \text{reaction_3}(X, Y). \\ \text{pathway}(X, Y) \leftarrow \text{reaction}(X, Y). \\ \text{pathway}(X, Y) \leftarrow \text{reaction}(X, Z), \\ \text{pathway}(Z, Y). \end{array} \right. \begin{array}{l} \mathbf{R}_1 \text{ (matrix)} : \begin{bmatrix} 0 & 0 & 0 & 1 & 1 \\ 0 & 1 & 1 & 0 & 0 \\ 1 & 0 & 0 & 0 & 0 \end{bmatrix} \\ \mathbf{R}_2 \text{ (matrix)} : \begin{bmatrix} 0 & 1 & 1 & 0 & 0 \\ 1 & 0 & 0 & 0 & 0 \\ 0 & 1 & 0 & 0 & 0 \end{bmatrix} \\ \mathbf{R}_1 \text{ (program)} : \begin{cases} v_1(1, 00011). \\ v_1(2, 01100). \\ v_1(3, 10000). \end{cases} \\ \mathbf{R}_2 \text{ (program)} : \begin{cases} v_2(1, 01100). \\ v_2(2, 10000). \\ v_2(3, 01000). \end{cases} \end{array}$$

Constant symbols are represented by rows in \mathbf{R}_1 and \mathbf{R}_2 . Constant symbols $c1_c2, c3_c4$ and $c5$ that appear on the left-hand side of reactions are denoted by binary bits in \mathbf{R}_1 . Constant symbols $c3, c4, c5$ and $c3_c4$ that appear on the right-hand side of reactions are denoted by binary bits in \mathbf{R}_2 . Each row in the boolean matrices is written as a unit ground clause. For example, since $\mathcal{P}_1 \models \text{reaction}(c1_c2, c3_c4)$, the first row of \mathbf{R}_1 is written a binary code "00011" to represent $c1_c2$ and the first row of \mathbf{R}_2 is a binary code "01100" to represent $c3_c4$. Each "1" binary bit indicates the presence of a constant symbol.

Each transformed program contains clauses describing an initial marking. These clauses are represented by a boolean vector \mathbf{v} which is a single-row boolean matrix where the binary bits correspond to the constant symbols.

Algorithm 1 Iterative extension (BMLP-IE)

Input: A $1 \times n$ vector \mathbf{v} , a $1 \times k$ vector \mathbf{t} that represents viable transitions, two $k \times n$ boolean matrices $\mathbf{R}_1, \mathbf{R}_2$ that encode unit ground clauses.

Output: Transitive closure \mathbf{v}^* .

```

1: Let  $\mathbf{v}^* = \mathbf{v}$ ,  $1 \times k$  vector  $\mathbf{v}' = \mathbf{0}$ .
2: while True do
3:   for  $1 \leq i \leq k$  do
4:      $(\mathbf{v}')_i = (\mathbf{t})_i$  if  $(\mathbf{v} \text{ AND } (\mathbf{R}_1)_{i,*}) == (\mathbf{R}_1)_{i,*}$ .
5:   end for
6:    $\mathbf{v}^* = (\mathbf{v}' \mathbf{R}_2) + \mathbf{v}$ .
7:    $\mathbf{v} = \mathbf{v}^*$  if  $\mathbf{v}^* \neq \mathbf{v}$  else break.
8: end while

```

Example 3 We show the mapping of a single row matrix from the token definition from \mathcal{P}_1 in Example 1. Individual substances are represented by constant symbols $c1$ and $c2$. The set of chemical substances is denoted by an additional concatenated constant symbol, $c1_c2$.

$$\mathcal{P}_1 : \left\{ \begin{array}{l} \text{token}(m1, c1_c2). \\ \text{token}(m1, c1). \\ \text{token}(m1, c2). \\ \dots \\ \text{reaction}(X, Y) \leftarrow \text{token}(X, Y). \\ \dots \end{array} \right. \quad \begin{array}{l} \mathbf{v} \text{ (vector)} : [0 \ 0 \ 0 \ 1 \ 1] \\ \mathbf{v} \text{ (program)} : \{v(1, 00011).\} \end{array}$$

On the right-hand side, the constant symbol $c1_c2$ is represented by the vector \mathbf{v} . Since the first token clause contains constant symbols in the other token clauses, \mathbf{v} only includes the right-hand side of the first token clause to avoid redundancy. In program form, \mathbf{v} is written as a unit ground clause containing a binary code "00011" to represent $c1_c2$.

The separation of this vector from \mathbf{R}_1 and \mathbf{R}_2 is meant to keep \mathbf{R}_1 and \mathbf{R}_2 static. Since the structure of the OEN does not vary often, we reduce the number of times that we need to re-create these two matrices while the definition of an initial marking usually changes across different simulations. We use all three created matrices, \mathbf{R}_1 , \mathbf{R}_2 and \mathbf{v} for bottom-up evaluation.

5.2 Iterative extension (BMLP-IE)

Given a program \mathcal{P} that contains a linear and immediately recursive clause r , we implement a BMLP algorithm called iterative extension to perform the bottom-up evaluation of r . The iterative extension algorithm (BMLP-IE) operates on two matrices to iteratively expand terms reachable in a partially grounded query $r(u, Y)$. Given that \mathcal{P} contains n constant symbols, we represent the constant symbols in u as a $1 \times n$ row vector or a n -bit binary code \mathbf{v} . Based on Section 5.1.1, we write $k \times n$ boolean matrices \mathbf{R}_1 and \mathbf{R}_2 for k unit ground clauses used by r . \mathbf{R}_1 and \mathbf{R}_2 describe which constant symbols appear first and second in the unit ground clauses. In addition, a $1 \times k$ boolean vector \mathbf{t} is used to express additional control on the

viability of transitions in the OEN. Transition can be turned “on” or “off” via this vector. “On” transitions have the binary value 1 and “off” transitions have the value 0. This allows us to temporarily modify the network connectivity without re-creating \mathbf{R}_1 and \mathbf{R}_2 .

We implement BMLP-IE (Algorithm 1) in SWI-Prolog (version 9.2) to compute the transitive closure of \mathbf{v} . In SWI-Prolog, each binary code can be written as an integer number, e.g. “00011” is the integer “3”. We use the bitwise AND to locate rows in \mathbf{R}_1 that contain all the 1 elements in \mathbf{v} . This computes indices of unit ground clauses that can extend the set of constant symbols in \mathbf{v} . These constants are added to \mathbf{v} via boolean matrix multiplication and addition. We iterate this process until we find the elements of \mathbf{v} no longer change.

Theorem 2 *Given a $1 \times n$ vector \mathbf{v} , a $1 \times k$ vector \mathbf{t} , two $k \times n$ boolean matrices \mathbf{R}_1 and \mathbf{R}_2 , Algorithm 1 has a time complexity $O(kn^2)$ for computing the transitive closure \mathbf{v}^* .*

Proof In Algorithm 1, the complexity of an iteration in the “while” loop is $O(k \times n)$ bitwise operations due to the multiplication between a vector and a $k \times n$ matrix. Each “for” loop pass also performs $O(k \times n)$ bitwise comparisons. Until we find the transitive closure, at least one unit ground clause needs to be added in each “while” loop iteration. Therefore, there are at most n iterations which require $O(k \times n^2)$ bitwise operations. \square

Theorem 2 shows that BMLP-IE has a polynomial runtime cubic in the size of the boolean matrices. Evaluating the program \mathcal{P} using SLD resolutions has the same time complexity and the runtime of BMLP-IE primarily benefits from bit-wise operations. For SLD resolutions, the size of the subset of the Herbrand base provable from a query $r(u, Y)$ is bounded by $O(n)$. Each member of this subset can be found via a depth-first search. Since there are k unit ground clauses and each variable can be grounded by at most n constants, this query requires at most n search in a tree of $O(k \times n)$ nodes. For OEN reachability queries, it is important to note that the size of boolean matrices grows linearly with the number of hypernodes because they are both bounded by the number of transitions.

6 Active learning

6.1 Hypothesis compression

We use the compression score of a hypothesis h to optimise the posterior probability. A learner can derive the relative frequency $p(h)$ for h to be chosen based on the encoding of h . In an optimal binary bit coding scheme [71], the length of h denoted by $size(h)$ is $-\log_2(p(h))$. The compactness of h ’s encoding reflects its prior probability $p(h) = 2^{-size(h)}$. We can use the compression function to compute the prior $p(h)$. Given a set of training examples E , the compression of a hypothesis [50,14] can be interpreted as

$$compression(h, E) = size(E) - MDL_{h,E}$$

In addition, the compression relates to the posterior probability of h [50]:

$$\frac{p(h|E)}{p(E|E)} = 2^{\text{compression}(h,E)}$$

We can re-arrange this to obtain the normalised posterior probability [14]:

$$p'(h|E) = \frac{2^{\text{compression}(h,E)}}{\sum_{h_i \in H} 2^{\text{compression}(h_i,E)}}$$

The posterior probability is maximal when compression is maximal. By searching for a hypothesis with maximum posterior probability, a learner can maximise its expected predictive accuracy [50]. To learn an accuracy hypothesis, the goal is to find a hypothesis with the highest compression score.

The compression function in $BMLP_{active}$ follows the Minimal Description Length (MDL) principle [19]. The most probable hypothesis h for the training examples E should be compact and have the fewest disagreements between E and predictions made by h . This minimises $L(h) + L(E|h)$, where $L(h)$ is the descriptive complexity of h and $L(E|h)$ is the descriptive complexity of encoding E using h . We consider a compression function from [14] based on the MDL principle:

$$\text{compression}(h, E) = |E^+| - \frac{|E^+|}{pc_h} (\text{size}(h) + fp_h)$$

where E^+ is the set of positive examples seen by the active learner, pc_h is the positive coverage by h and fp_h is false positives covered by h . In other words, this compression function favours a general hypothesis with high coverage and penalises over-general hypotheses that incorrectly predict negative examples. The generality of h can be estimated by computing its coverage pc_h for a set of unlabelled instances [50]. To determine the hypotheses' compression scores, $BMLP_{active}$ looks at all available experiment instances to obtain a good estimate of a hypothesis's generality. Learning with increasingly large hypothesis space and instance space thus requires efficient inferences in the background knowledge. Our BMLP approach addresses this by manipulating boolean matrices for bottom-up evaluations.

6.2 Expected cost of experiments

Experiment planning is often restricted by time and other resources. A rule of thumb for experiment design is to achieve optimal empirical outcomes within a finite budget. The problem of designing experiments to support or refute scientific hypotheses involves a series of binary decisions. This process is analogous to playing the game of "Guess Who" where players ask a sequence of "yes" or "no" questions whose answers binarily partition the candidate hypotheses. The outcome of an experiment t splits hypotheses H into consistent hypotheses H_t and inconsistent hypotheses \overline{H}_t . The path of selection and outcomes of experiments can be represented as a binary decision tree. To construct an optimal tree, an active learner should seek to label instances consistent with up to half of the hypotheses [47].

In addition to this principle, we consider a user-defined experiment cost function C_t of experiment t . The experiment selection is represented by a binary tree with paths annotated by the costs of experiments. The optimal selection is therefore a

binary tree with the minimum expected overall cost. The minimum expected cost of performing a set of candidate experiments T can be recurrently defined as:

$$EC(\emptyset, T) = 0$$

$$EC(h, T) = 0$$

$$EC(H, T) = \min_{t \in T} [C_t + p(t)EC(H_t, T - t) + (1 - p(t))EC(\overline{H}_t, T - t)]$$

To estimate this recurrent cost function, $BMLP_{active}$ uses the following heuristic function from [14] to approximate optimal cost selections:

$$EC(H, T) \approx \min_{t \in T} [C_t + p(t)(\text{mean}_{t' \in T - \{t\}} C_{t'})J_{H_t} + (1 - p(t))(\text{mean}_{t' \in T - \{t\}} C_{t'})J_{\overline{H}_t}]$$

where $p(t)$ is the probability that the outcome of the experiment t is positive and $J_H = -\sum_{h \in H} p(h) \log_2(p(h))$. The probability $p(h)$ is the prior of hypothesis h calculated from the compression function. To estimate $p(t)$, we compute the sum of the probabilities of the hypotheses consistent with a positive outcome of t . While we only focus on auxotrophic mutant experiments in this work, users can flexibly define the experiment cost function for different types of experiments.

6.3 Active learning sample complexity

For some hypothesis space H and background knowledge BK , let V_s denote the version space of hypotheses consistent with s training examples. For an active version space learner that selects one instance per iteration, $|V_s|$ denotes the size of the version space at the iteration s of active learning. The shrinkage of the hypothesis space can be represented by the reduction ratio $\frac{|V_{s+1}|}{|V_s|}$ after querying the label of the s -th instance [36]. The minimal reduction ratio $p(x_s, V_s)$ is the minority ratio of the version space V_s partitioned by an instance x_s .

Definition 4 (Minimal reduction ratio [36]) The minimal reduction ratio over the version space V_s by sampled instance x_s is

$$p(x_s, V_s) = \frac{\min(|\{h \in V_s | h \cup BK \models x_s\}|, |\{h \in V_s | h \cup BK \not\models x_s\}|)}{|V_s|}$$

The minimal reduction ratio of an actively selected instance can be computed before it is labelled. While in reality training examples might not be as discriminative, the optional selection strategy is to select instances with minimal reduction ratios as close as possible to $\frac{1}{2}$ with the ability to eliminate up to 50% of the hypothesis space. We describe the sample complexity advantage of active learning over random example selection by the following bound of an active version space learner's sample complexity. A passive learner is considered a learner using random example selection since it does not have control over the training examples it uses.

Theorem 3 (Active learning sample complexity bound) For some $\phi \in [0, \frac{1}{2}]$ and small hypothesis error $\epsilon > 0$, if an active version space learner can select instances to label from an instance space \mathcal{X} with minimal reduction ratios greater than or equal to ϕ , the sample complexity s_{active} of the active learner is

$$s_{active} \leq \frac{\epsilon}{\epsilon + \phi} s_{passive} + c \quad (2)$$

where c is a constant and $s_{passive}$ is the sample complexity of learning from randomly labelled instances.

Proof We consider an arbitrary distribution of the minimal reduction ratio over \mathcal{X} bounded by $[0, \frac{1}{2}]$. Suppose a version space learner can select instances with a minimal reduction ratio greater than ϕ . Since ϕ represents the ratio of the minority partition, the number of candidate hypotheses remaining in the version space V_s after s labelled instances is bounded by the size of the majority partitions $(1 - \phi)^s |H|$ where H is the hypothesis space. The probability that any hypothesis in V_s with an error larger than ϵ is consistent with s training examples is:

$$\begin{aligned} p_{error} &= (1 - \epsilon)^s |V_s| \\ &\leq (1 - \epsilon)^s (1 - \phi)^s |H| \end{aligned}$$

p_{error} should be small so suppose for small $\delta > 0$,

$$(1 - \epsilon)^s (1 - \phi)^s |H| = \delta \quad (3)$$

Equation 3 corresponds to the probability of the extreme case when only the minority of the remaining hypotheses can be eliminated by each labelled instance. By rearranging Equation (3), the number of training examples required by this learner in this extreme case is:

$$s = \frac{1}{-\ln(1 - \epsilon) - \ln(1 - \phi)} (\ln(|H|) + \ln(\frac{1}{\delta}))$$

For an arbitrary active learner whose membership queried instances also have a minimal reduction ratio greater than or equal to ϕ , the number of actively selected instances s_{active} is upper bounded by s for reducing the size of version space to $|V_s|$. Since $(1 - u) < e^{-u}$ for small $u > 0$, it is true that $-\ln(1 - u) > u$. So the following holds:

$$s_{active} < \frac{1}{\epsilon + \phi} (\ln(|H|) + \ln(\frac{1}{\delta}))$$

According to the Blumer bound [10], for a version space learner that randomly samples examples to produce a hypothesis of error at most ϵ with a probability less than or equal to δ , the sample complexity is $s_{passive} > \frac{1}{\epsilon} (\ln(|H|) + \ln(\frac{1}{\delta}))$. Following this, it must be true that $\epsilon s_{passive} > (\epsilon + \phi) s_{active}$. So we can derive the Inequality 2 in the theorem:

$$s_{active} \leq \frac{\epsilon}{\epsilon + \phi} s_{passive} + c$$

where c is a constant. \square

This theorem shows the sample complexity gain of active learning over learning from randomly sampled instances. Theorem 3 says that the number of instances needed to select by active learning should be some factor smaller than the number of randomly sampled examples given some predictive accuracy level. Given a desirable predictive error ϵ , this factor can be computed if the minimal reduction ratio ϕ can be estimated from the instance space. When selected instances have a larger minimal reduction ratio, the sample complexity gain would be more significant. On the other hand, if instances have low discriminative power and the minimal reduction ratio tends to zero, the sample complexity gain would be minimal. In Section 8, we empirically show empirical evidence supporting this theorem for $BMLP_{active}$ and randomly sampled experiments when learning gene functions in a GEM.

iML1515 separates metabolites into different compartments in the cell. The suffices “e” (extracellular space) and “c” (cytosol) represent two compartments, which divide the metabolic network into sub-networks.

Our encoding of the GEM *iML1515* also contains *codes/2* and *enzyme/6* definitions. These clauses enable us to describe metabolic reactions via boolean matrices. We convert gene-reaction-metabolite mappings and standard identifiers in *iML1515*¹ into a logic program containing *codes/2* and *enzyme/6* clauses. *iML1515* uses standard nomenclature so the logic program encoding can be applied to other genome-scale metabolic networks. The logic program encoding can also be linked to publications and external databases to obtain further details on genes, proteins, reactions and metabolites.

7.2 Simulating a GEM using BMLP-IE

Algorithm 2 BMLP phenotype prediction

Input: Background knowledge BK , an experiment query q .

Output: A binary phenotypic effect classification: 1 represents a phenotypic effect and 0 denotes no phenotypic effect.

- 1: From *reaction/2* clauses in BK , create boolean matrices $\mathbf{R}_1, \mathbf{R}_2$.
 - 2: From biomass metabolites in BK , create vector $\mathbf{v}_{biomass}$.
 - 3: From growth medium metabolites in q , create vector \mathbf{v} .
 - 4: From knockout genes in q , create vector \mathbf{t} for viable reactions.
 - 5: return 1 if (BMLP-IE($\mathbf{v}, \mathbf{t}, \mathbf{R}_1, \mathbf{R}_2$) AND $\mathbf{v}_{biomass} \neq \mathbf{v}_{biomass}$) else return 0.
-

To simulate the GEM *iML1515* using BMLP-IE, *reaction/2* clauses are created from *enzyme/6* clauses. Each clause contains reactants and product identifiers. Each reversible reaction is defined as two clauses where reactants and products are swapped. One difference between *BMLP_{active}* and the Robot Scientist is that *BMLP_{active}* allows multiple gene deletions, e.g. *phenotypic_effect([b2290, b2379], [glyc_e])*. This enables the learning of digenic interactions such as gene-isoenzyme functions. Since multiple genes can be responsible for the same enzyme, single knockouts may not have phenotypic effects. A hypothesis of a gene-isoenzyme function contains one *codes/2* clause and one *enzyme/6* clause. The *enzyme/6* in the hypothesis would be a replicate of an existing clause in the background knowledge with a new enzyme identifier.

Another difference is that boolean matrices are created using the *reaction/2* clauses for bottom-up evaluation. Algorithm 2 shows the application of BMLP-IE (Algorithm 1) for finding the transitive closure of synthesisable substances. The two boolean matrices inputs to the BMLP-IE algorithm represent reactants and products participating in the reactions. The growth medium condition is encoded as the input vector to the BMLP-IE algorithm. This vector would be extended to represent substances that are synthesisable by the organism in an auxotrophic mutant experiment. Specifying knockout genes excludes a subset of reactions. A vector computed during

¹ The *iML1515* model is described in the text-based JavaScript Object Notation (JSON). It uses standard identifiers from the Biochemical Genetic and Genomic (BiGG) [40] knowledge base of large-scale metabolic reconstructions.

an intermediate step in the BMLP-IE algorithm denotes viable reactions given the set of knockout genes. A viable reaction is indicated by a binary bit 1 in this vector. Blocked reactions are excluded based on *codes/2* and *enzyme/6* definitions. In BMLP-IE, boolean operations compute the transition between metabolic states and return the closure set of synthesisable substances. A binary phenotypic classification is made according to the inclusion of essential substances in the closure set, indicating cell growth comparable to an unedited wild-type MG1655 *E. coli* strain. A binary classification of “1” corresponds to a phenotypic effect and “0” is no phenotypic effect. The essential substances come from the biomass function of the wild-type in iML1515 [48]². The biomass function describes the necessary substance composition for the growth of the organism.

7.3 Active learning using BMLP

Algorithm 3 *BMLP_{active}*

Input: Hypotheses H , background knowledge BK , experiment instances T , experimental cost budget C , total number of experiment N and oracle O .

Output: A hypothesis $h_{max} \in H$.

```

1: Let  $T_{selected} = \emptyset$ ,  $V_0 = H$ .
2: while  $cost(T_{selected}) \leq C$  and  $|V_j| > 1$  and  $|T_{selected}| < N$  do
3:   if  $T_{selected} == \emptyset$  then
4:     Select  $t_j$  with the largest minimum reduction ratio  $p(t_j, V_j)$ 
5:     from remaining experiments in  $T$  to add to  $T_{selected}$ .
6:   else
7:     Add experiment  $t_j \in T$  that has the minimum cost  $EC(V_j, T')$  to  $T_{selected}$ .
8:   end if
9:   break if  $cost(T_{selected}) > C$ 
10:  Consult the label  $l$  of  $t_j$  from the oracle  $O$ .
11:   $\mathbf{R}_{i,j} = BMLP\_phenotype\_prediction(h_i \cup BK, t_j)$  for all  $h_i \in V_j$ 
12:   $V_{j+1} = \{h_i \mid h_i \in V_j \text{ and } \mathbf{R}_{i,j} = l\}$ .
13:  For  $h_i \in V_{s+1}$ , compute  $compression(h_i, T_{selected})$ .
14:   $h_{max}$  is the hypothesis with the largest compression score.
15: end while

```

Active learning in *BMLP_{active}* is described by Algorithm 3. The input background knowledge is created from a GEM model. The user needs to provide a set of candidate experiments, candidate hypotheses and an experiment cost function. Labels of experiment instances are requested from a data source, e.g. a laboratory or an online dataset. Labelled experimental data are considered ground truths. Initially, we randomly shuffle all candidate experiments and select an experiment with the most discriminative power if its cost is under budget. Alternatively, a discriminative experiment with the lowest cost can be selected for a fixed initialisation.

In each active learning cycle in *BMLP_{active}*, hypotheses inconsistent with ground truth experimental outcomes are pruned. *BMLP_{active}* selects experiments to minimise the expected value of a user-defined cost function (see Section 6). We apply

² We use the wild-type biomass function specified by iML1515 from <http://bigg.ucsd.edu/> [40]. We use the qualitative version of this biomass function, meaning that we only care about the substances in the biomass, not their reaction coefficients.

BMLP-IE to obtain predicted experiment outcomes and compare them with experimental data. For a hypothesis space H and a set of experiment instances T , BMLP-IE produces predicted outcomes in a boolean matrix \mathbf{R} of size $|H| \times |T|$. Given the j -th actively selected instance $t_j \in T$ and $h_i \in V_j \subseteq H$, $(\mathbf{R})_{i,j} = 1$ if $h_i \cup BK \models t_j$ and otherwise $(\mathbf{R})_{i,j} = 0$. We refer to \mathbf{R} as a classification table. In experiments from Section 8, we construct classification tables by predicting phenotypic effects for all combinations of candidate experiments and hypotheses. This avoids repeating simulations in hypothesis pruning and compression calculation. When computing hypothesis compression, we estimate the generality of a hypothesis by calculating its coverage for all unlabelled instances based on the classification table. Currently, we only consider labels from synthetic or online phenotype data. However, $BMLP_{active}$ can be coupled with a high-throughput experimental workflow to automate experiments.

8 Experiments

Since a logic program representing a GEM describes many biological entities and intricate relations between them, abduction of gene function hypotheses and in-vivo validations requires exploring a large hypothesis space and instance space. Both are challenging computationally and empirically. $BMLP_{active}$ aims to address these by evaluating a large logic program with boolean matrices and actively selecting experiment instances to perform. In our experiments³, we intend to demonstrate that the $BMLP_{active}$ framework can efficiently perform phenotypic predictions and actively suggest informative experiment instances that can reduce experiment costs.

In this work, we define the experimental cost function as the cost of the reagents which are optional nutrient substances used in selected experiments. We also assume when added to growth media, reagents are used in the same volume. In addition, we do not explicitly account for plastic consumables, equipment depreciation or specify the time to carry out each experiment, which we consider fixed and are affected mainly by the number of experiments. We also do not account for costs incurred due to different experiment types such as different measurement timescales that prevent experiments from being performed concurrently. To maintain consistent scaling for comparisons, the total experimental reagent cost is the amount of unit cost required by selected experiments. We consider the unit cost of the reagents as the cost of the cheapest reagent. We calculate the total experimental reagent cost as the sum of the reagent costs⁴ in selected experiments divided by the unit cost.

Q1: Can BMLP-IE reduce the runtime of simulating GEM?

Using only Prolog to simulate metabolic networks requires grounding viable reaction pathways based on SLD resolutions. We aim to demonstrate that a general-purpose Prolog interpreter can be augmented with our BMLP approach for faster phenotypic simulations given logically encoded metabolic network models. $BMLP_{active}$ extends the logical representation of a metabolic network in the Robot Scientist [39,

³ All experiments are performed on a workstation with Intel(R) Core(TM) i9-7900X CPU 3.30GHz (20 CPUs).

⁴ We provide the costs of reagents in Table 2 and 3 of Appendix A.

14] by additionally applying boolean matrix computation via BMLP. Therefore, we consider the Robot Scientist’s logical encoding as a benchmark. Since the Robot Scientist was implemented using Prolog [50], we adapt its metabolic network encoding to SWI-Prolog. To answer **Q1**, we compare the simulation runtime of $BMLP_{active}$, which uses SWI-Prolog and BMLP-IE, against the Robot Scientist’s encoding in SWI-Prolog.

Q2: Does BMLP-IE accurately predict phenotypes?

BMLP-IE makes binary phenotypic predictions and accounts for the necessary growth conditions of the organism. In contrast to qualitative predictions produced by BMLP-IE, FBA [56] is more commonly used in the literature to quantitatively predict the cell growth rate based on fluxes of biomass metabolites at the steady state. We compare BMLP-IE phenotypic predictions against those given by FBA from the iML1515 model in [48]. To answer **Q2**, the comparison between BMLP-IE and FBA predictions is made with respect to ground truth experimental data also in [48].

Q3: Can $BMLP_{active}$ reduce the cost for learning gene functions in GEM?

We consider two measures of experiment cost: the experimental resource cost and the number of experiments. These two costs are related since the number of experiments generally is the main driver of experimental cost. We aim to show that experiments selected by $BMLP_{active}$ reduce overall experimental reagent cost compared to random experiment selection. We additionally demonstrate that $BMLP_{active}$ lowers the number of experiments (the sample complexity) needed to learn accurate gene functions. Gene function recovery experiments are conducted to answer **Q3**. To demonstrate that $BMLP_{active}$ can recover known gene functions, we delete parts of iML1515 to create an incomplete knowledge base artificially. Active learning from the incomplete model is a mock of an actual discovery. Active learning aims to recover deleted gene functions within a reagent cost budget and with a limited number of experiments. We also examine **Q3** for recovering isoenzyme functions which require navigating a large experimental design space.

Q4: Does Theorem 3 correctly describe the relationship between the sample complexity of $BMLP_{active}$ and random experiment selection?

Theorem 3 shows the advantage of active learning in improving the efficiency of experimentation. We empirically examine the sample complexity bound specified in Theorem 3. Let the sample complexity of $BMLP_{active}$ and a random experiment sampling learner be s_{active} and $s_{passive}$ respectively. From Theorem 3 we can obtain the following inequality:

$$\frac{\epsilon}{s_{active}} \geq \frac{\epsilon + \phi}{s_{passive}} + c \text{ with } c \text{ as constant}$$

In order to answer **Q4**, we use $BMLP_{active}$ and random experiment sampling to recover gene functions as described above. We calculate the ratios of the error rates of learned gene functions over the number of experiments selected.

	Single thread (seconds)	20 CPUs (seconds)
SWI-Prolog	37.842 ± 9.668	5.089 ± 0.119
SWI-Prolog + BMLP-IE	0.220 ± 0.099	0.061 ± 0.008

Table 1: Simulation runtimes in CPU time. BMLP-IE leads to a 170 times improvement in simulation time efficiency. Multi-threading BMLP-IE enhances runtime efficiency 600 times compared to base SWI-Prolog.

Q5: Can $BMLP_{active}$ learn digenic interactions?

While isoenzyme functions are identified as one source of errors in iML1515 [9], full exploration of the gene-isoenzyme relations is laborious. This motivates us to answer **Q5**. We perform gene function recovery experiments using $BMLP_{active}$ to rediscover a key isoenzyme for demonstration. We focus on the aromatic amino acid biosynthesis pathway. It is a critical pathway for micro-organism survival that contains important gene targets for engineering high aromatic amino acid production strains. Although this pathway has been intensively studied for decades, gaps remain in the understanding of gene-gene relations [59]. We show that an isoenzyme function in the aromatic amino acid pathway can be accurately recovered via active learning. This demonstrates when $BMLP_{active}$ is integrated with an experimental workflow that systematically perturbs genes under different growth conditions, we can potentially reveal novel insights for metabolic engineering and strain optimisation.

8.1 Experiment 1: BMLP-IE simulations and predictions

Materials. In each simulation, we used $BMLP_{active}$ to predict a phenotype in an auxotrophic single-knockout mutant experiment. Every experiment removes one gene from the biological system and uses a growth medium. The GEM iML1515 has been validated against 16 carbon sources as optional nutrients in [48]. We focused on the same experimental conditions for simulations with base SWI-Prolog and $BMLP_{active}$. Experimental phenotypic data on the same 16 carbon sources and FBA phenotypic predictions of iML1515 are already processed as binary classes in [48]. In [48], measured and predicted mutant growth rates at a proportion of the wild-type’s growth rate greater than a fixed threshold are mapped to the no phenotypic effect class.

Methods. We randomly sampled 100 simulations to perform and compute the average wall time for each computation method. We first compared the mean and standard deviation in simulation time of our new logical matrix encoding against the Prolog encoding. In addition, we explored multi-threading with both encodings. We used the multi-threading library offered by SWI-Prolog. Owing to the overhead of managing threads, multi-threading boolean operations with SWI-Prolog have diminishing returns. In BMLP-IE, simulation parameters are encoded as matrices, enabling us to run simulations in batches. For BMLP-IE, we used the concurrent threading library

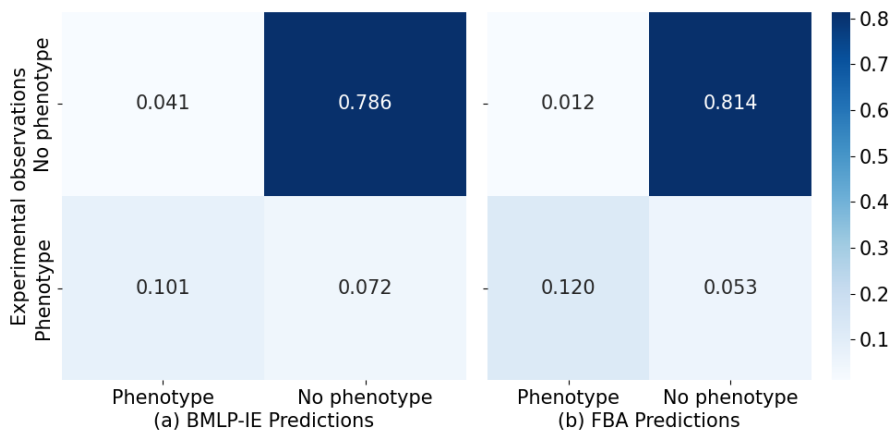


Fig. 4: Normalised confusion matrices of (a) BMLP-IE and (b) FBA phenotypic predictions based on the GEM model iML1515. Each number has been normalised by the size of the experiment dataset in [48]. From this dataset, the phenotypic prediction accuracies of BMLP-IE and FBA are 88.7% and 93.4% respectively.

in SWI-Prolog at the batch level. The runtime experiments with the multi-threading are repeated 10 times. We show this comparison in Table 1.

To evaluate BMLP-IE’s accuracy, we compared its phenotypic predictions against experimental phenotypic data on the same 16 carbon sources. We identified the number of consistent and inconsistent predictions and created normalised confusion matrices for BMLP-IE and the FBA predictions from [48]. We show these normalised confusion matrices in Fig 4.

Results and discussion. Table 1 shows a 170 times improvement in simulation time by BMLP-IE compared to base SWI-Prolog. The simulation runtime is further improved with multi-threading. With 20 cores, BMLP-IE uses only $\frac{1}{600}$ of the simulation time compared to running simulations with base SWI-Prolog. However, the multi-threading runtime improvement is not as pronounced as the runtime improvement from using BMLP-IE. This result answers **Q1** as the SWI-Prolog implementation of BMLP-IE significantly improves the phenotype simulation runtime of iML1515. While BMLP-IE is a specific-purpose algorithm, this result shows that a machine learning system implemented in SWI-Prolog can be more time-efficient if it uses BMLP-IE when the background knowledge can be described as a linear and immediately recursive datalog program.

In Fig 4, the confusion matrices show a comparable predictive accuracy by BMLP-IE (88.7%) to that of standard FBA (93.4%). This answers the question **Q2**. Compared with FBA’s growth rate predictions, the misclassifications by BMLP-IE are mainly due to it not being able to predict reduced cell growth. FBA permit quantitative descriptions of metabolic fluxes but metabolites are only binarily represented in an OEN. However, the strength of the BMLP-IE approach is that it is easily adaptable for extending the underlying GEM. FBA methods are mainly used

as mathematical modelling tools so they are not immediately applicable for learning.

8.2 Experiment 2: active learning sample complexity and experiment cost

Materials. Up to 3 of 16 common carbon sources were used as additional nutrients to the base growth medium. Each of these 16 carbon sources is an optional nutrient in the experimental data for validating [48]. This set contains preferred carbon sources [45,82] for *E. coli* such as glucose and glycerol. We first simulated iML1515 with up to 3 optional carbon sources, generating $\sum_{i=0}^3 \binom{16}{i} = 697$ synthetic data. This allows us to go beyond the 16 experimental data for each gene knockout in [48]. We observed a single-knockout phenotypic effect from 213 genes. We treated these synthetic data as ground truths where 213 genes have only positive examples. We only focused on a subset of 2 genes because they have both positive and negative examples⁵. Then, we removed gene functions associated with these 2 genes from the background knowledge. Thus, the resulting incomplete model has a smaller set of *codes/2* clauses.

Methods. We focused on one removed gene function at a time to recover it. Each hypothesis except the empty hypothesis associates a gene locus identifier, whose function we tried to recover, with an *enzyme/6* clause. We concentrate on 1294 *enzyme/6* clauses that represent the non-maintenance reactions in iML1515. Therefore, the hypothesis space had 1295 *codes/2* hypotheses, including an empty hypothesis. The instance space contained 697 experiments with optional growth nutrients up to 3 carbon sources.

BMLP_{active} actively selected experiments from the instance space to reduce the hypothesis space. The random selection method randomly sampled instances from the instance space. First, we constrained the selection of experiments by an experimental reagent cost budget C . After experiment selection, both methods returned the hypothesis with the single highest compression, otherwise, a hypothesis was selected from those sharing the highest compression randomly. The final hypotheses obtained by either method would output a recovered model. We compared *BMLP_{active}* with the random experiment selection strategy with increasing experimental reagent cost budget $C \in \{1, 10, 50, 100, 500, 1000, 5000, 10000\}$. We tested the predictive accuracy of the recovered models against all 697 synthetic data. The cost of selected experiments and predictive accuracy of the recovered model were recorded for *BMLP_{active}* and random selection. Each selection method was repeated 10 times for each reagent cost budget C . We show this comparison in Fig 5.

In addition, we constrained the number of experiments N that can be selected by increasing it linearly according to $\{0, 1, 2, 3, 4, 5, 10, 15, 20, 25, 30\}$. We applied *BMLP_{active}* and random experiment selection with compression to decide the final hypothesis for recovering models. Each selection method was repeated 10 times for every number of selected experiments N . Then, we computed the phenotypic predictive accuracy of the recovered models against all 697 synthetic data. We show this comparison in Fig 6. For experiment number limits excluding 0, we calculated

⁵ The distribution of training examples for this experiment is described in Table 4 of Appendix B.

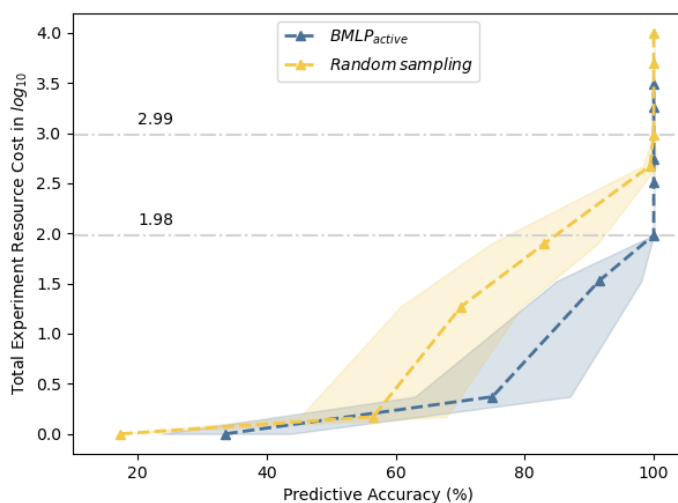


Fig. 5: Total experimentation cost needed for the recovered models to reach different levels of predictive accuracy. Models recovered from random experiment selection and $BMLP_{active}$ can both converge to 100% predictive accuracy. However, models recovered by $BMLP_{active}$ reach 100% predictive accuracy with $\frac{1}{10}$ reagent cost expenditure of random experiment sampling. The predictive accuracy of an empty hypothesis is 17.4%.

the mean error of learned hypotheses and divided it by the number of experiments selected to obtain the ratio. In Fig 7, we demonstrate how these ratios change to support Theorem 3.

Results and discussion. Fig 5 shows that $BMLP_{active}$ spends 10% of the cost used by random experiment sampling when converging to the correct hypothesis. The y-axis is the total experimental reagent cost in \log_{10} calculated from selected experiments. And 100% predictive accuracy indicates successful recovery of the deleted gene functions. The correct gene functions were recovered by $BMLP_{active}$ and random experiment selection with $10^{1.99}$ and $10^{2.99}$ experimental reagent costs respectively. The total experimental reagent cost is computed by dividing the unit cost which is the cost of the cheapest optional nutrient ($\pounds 0.038/gram$). Given the current hypothesis space and experimental design space and assuming each reagent was used one gram, experiments selected by $BMLP_{active}$ and random sampling would cost $10^{1.99} \times 0.038 \approx \pounds 3.8$ and $10^{2.99} \times 0.038 \approx \pounds 38$ to learn a single gene function. Consideration of differential resource factors in the user-defined experimental cost function could significantly increase the total experimental cost.

We then examined the advantage of $BMLP_{active}$ over random experiment selection on the number of experiments needed to recover gene functions. The number of experiments is a significant determinant of experimental cost. Fig 6 shows that $BMLP_{active}$ reduces the number of instances needed for labelling to learn accurate gene functions. While random experiment selection requires 25 experiments to re-

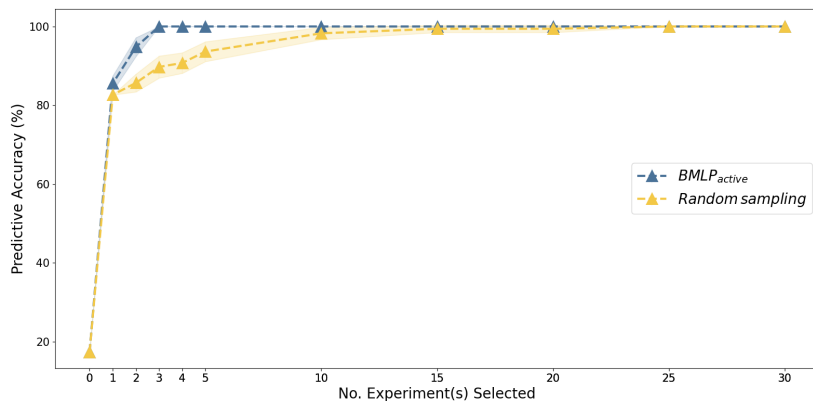


Fig. 6: Reduction of the number of experiments needed to recover gene functions (sample complexity reduction). *BMLP_{active}* learns 100% accurate gene functions with 3 experiments while random sampling requires 25 experiments to do so. The predictive accuracy of an empty hypothesis is 17.4 %. Predictive accuracy is higher for both methods initially since experiment selection is no longer constrained by reagent costs.

cover the deleted gene functions, *BMLP_{active}* only needed 3 experiments. Fig 5 and Fig 6 answer the question **Q3** since *BMLP_{active}* successfully reduced the experimental reagent cost and experiment cost compared to random experiment selection. Fig 5 and Fig 6 show *BMLP_{active}* can simultaneously optimise a user-defined experimental cost function and reduce the total number of experiments to learn gene functions accurately. This means that *BMLP_{active}* is highly flexible and could be tailored for specific experimental objectives in a discovery process. Later, in Experiment 3, we revisit the question **Q3** for recovering a known gene-isoenzyme association which presents a bigger empirical challenge due to the need to explore a larger experimental design space.

Fig 7 demonstrates the mathematical relationships between predictive error and the number of experiments required by *BMLP_{active}* and random experiment selection to converge to the correct hypothesis. For this gene function recovery task, *BMLP_{active}* selected experiments with minimal reduction ratio $\phi \geq 0.5\%$. The ratio $\frac{\epsilon}{s_{active}}$ is greater than $\frac{\epsilon + \phi}{s_{passive}}$ for error $\epsilon > 0$. There are fewer points on the active learning ratio curve since *BMLP_{active}* converges to 100% accuracy using fewer training examples. The two curves intersect at $\epsilon = 0$ since both converged to 100% accuracy. Fig 7 answers the question **Q4** and supports Theorem 3. Theorem 3 shows that active learning (*BMLP_{active}*) can reduce the requirement for training examples compared with passive learning (random experiment selection) to achieve a certain learning performance. In the context of scientific discovery, the experimental cost to arrive at a finding can be reduced by active learning since each actively selected experiment can have a higher return of information.

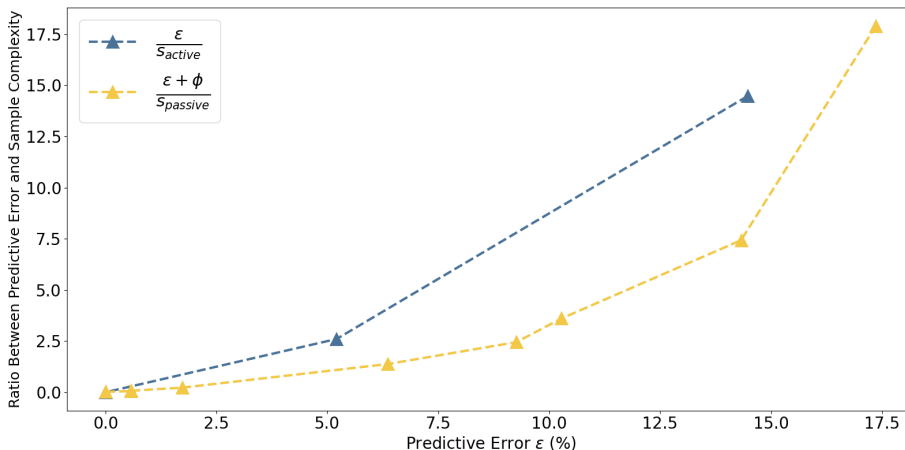


Fig. 7: Ratio of sample complexity. $BMLP_{active}$ selects instances with a minimal reduction ratio of at least 0.5%. For error $\epsilon > 0$, the ratio of $BMLP_{active}$ is clearly above the ratio of random sampling. This shows that Theorem 3 correctly describes the sample complexity relationship between active learning and random sampling.

8.3 Experiment 3: learning digenic functions

Materials. We focused on re-discovering a target isoenzyme function associated with the gene *tyrB* in the Tryptophan biosynthesis pathways. We aim to demonstrate gene-isoenzyme function learning by recovering this gene function. Associated functions of *tyrB* and *aspC* can be classified as isoenzyme functions since they are responsible for producing an important amino acid L-phenylalanine. In our logical representation of iML1515, we use reaction and *codes/2* unit ground literals to describe an isoenzyme. We selected 33 genes associated with this essential pathway. In this focus gene set, 27 genes are associated with a single function and 6 genes are related to two functions. We consider medium conditions with 7 optional nutrients including aromatic amino acids for recovering the deleted *tyrB* isoenzyme function. Aromatic amino acids are fundamental for protein synthesis but also serve as precursors for vital secondary metabolites and high-value chemicals [16].

Methods. We removed *tyrB*'s gene function and metabolic reaction associated with this isoenzyme from $BMLP_{active}$. The experiment instance space contained double gene-knockout and single gene-knockout experiments of 33 genes. There were $\binom{33}{2}$ gene pair combinations for double-gene knockout experiments and 33 single-gene knockout experiments. We considered growth medium conditions with the 7 optional nutrients. Therefore, the experiment instance space was $(\binom{33}{2} + 33) \times 7 = 3927$ and 3696 experiment instance labels were synthetically generated from double-knockout experiments using the full iML1515 background knowledge. The rest 231 single-knockout empirical data were from validation data in [48].

In the metabolic network, an isoenzyme function hypothesis contains a node represented by a new enzyme identifier (a *enzyme/6* clause) and a new link between a gene locus identifier and this new enzyme identifier (a *codes/2* clause). The hy-

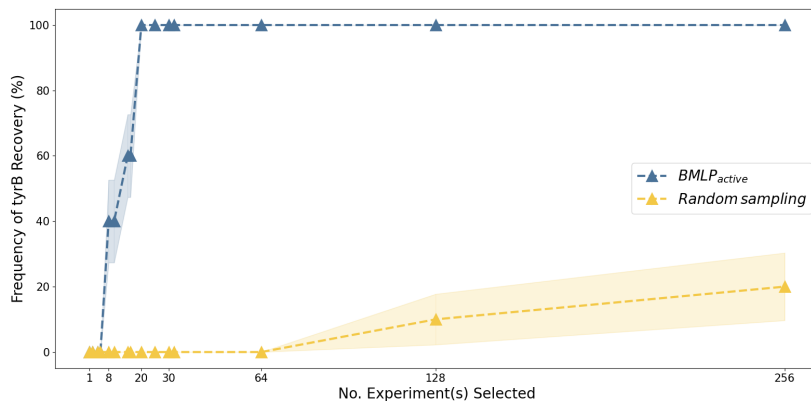


Fig. 8: tyrB isoenzyme function recovery frequency. We obtain the frequency of successful recovery from various randomisation seeds and compute the standard errors. We observe that within 64 experiments, random experiment selection does not recover the tyrB isoenzyme function. In contrast, $BMLP_{active}$ can recover this function with high frequency with 20 experiments.

pothesis space contained associations of 33 genes (from the focused library) with 33 *enzymes*/6 clauses. There were $(27 \times 32 + 6 \times 31) = 1050$ potential hypotheses for 27 single-function genes and 6 double-function genes. We also included the tyrB function hypothesis and an empty hypothesis, which gave 1052 hypotheses in total. We increased linearly and exponentially the number of experiments N that could be selected according to $\{1, 2, 4, 5, 8, 10, 15, 16, 20, 25, 30, 32, 64, 128, 256\}$. $BMLP_{active}$ selected N experiments from this instance space to actively learn from the hypothesis space. The random selection strategy randomly sampled N instances from the instance space. Again, both methods output the hypothesis with the highest compression according to the sampled examples. A hypothesis was randomly selected when multiple competing hypotheses shared the highest compression. We recovered the models by adding the final hypotheses. We recorded the number of experiments selected and evaluated if the recovered models contained the target isoenzyme function from the iML1515 background knowledge. Each experiment selection method was repeated 10 times and we computed the frequency of successful isoenzyme recovery across these 10 repeats. We show this comparison in Fig 8.

Results and discussion. Fig 8 shows the result of recovering tyrB’s isoenzyme function. For answering question **Q5**, we observed that $BMLP_{active}$ successfully recovers the correct tyrB isoenzyme function in 20 experiments. This demonstrates $BMLP_{active}$ ’s ability to discover gene-isoenzyme associations in GEM. However, to learn all isoenzyme functions, a high-throughput experimentation procedure is required and we further discuss this in Section 9.

This result also shows that $BMLP_{active}$ significantly reduced the number of experiments needed compared to random experiment selection, which answers the question **Q3**. $BMLP_{active}$ provides higher information gain from each experiment and can guarantee recovery with as few as 20 experiments. While random sampling

could prune most candidate hypotheses, it failed to eliminate competitive hypotheses further. In contrast to $BMLP_{active}$, random sampling could not recover this isoenzyme function with 64 experiments and could only do this occasionally with more than 10 times the number of experiments required by $BMLP_{active}$. Although we used a reduced set of genes in this demonstration, the combinatorial space was sufficiently large that random experiment selection became non-viable as an experimentation strategy in a discovery process. The remarkable increase in efficiency with $BMLP_{active}$ with this task demonstrates it has potential even as the experimental design space grows.

9 Conclusion and future work

We present a new logic programming system $BMLP_{active}$ that can simulate and learn gene functions in a state-of-the-art GEM. This GEM, iML1515, describes 1515 genes and 2719 metabolic reactions in *E. coli*. To our knowledge, $BMLP_{active}$ is the first logic programming system able to operate on GEMs. We implement $BMLP_{active}$ via our proposed BMLP approach by exploiting boolean matrices to improve the simulation runtime of a GEM by 170 times. Our empirical results show that $BMLP_{active}$ can learn gene functions while reducing the cost of optional nutrient substance in experiments by 90%. In addition, we deploy $BMLP_{active}$ to actively learn gene-isoenzyme functions which are an error source in GEM. As a demonstration, we empirically show that $BMLP_{active}$ can learn an important isoenzyme function in the aromatic amino acid biosynthesis pathway with as little as 20 training examples. In comparison, random experiment selection cannot learn this isoenzyme function consistently even with more than 250 training data. $BMLP_{active}$ provides a substantial advantage for isoenzyme function discovery over random experiment selection due to the sample complexity reduction. This finding suggests that $BMLP_{active}$ could be used to offset the growth in experimental design spaces associated with genome-scale function learning.

One limitation of $BMLP_{active}$ is that it cannot yet quantitatively predict the behaviours of biological systems. Quantitative growth predictions would allow us to model in-vivo phenotype observations without binary discretisation. Future work will focus on using logic programs to optimise relations and parameters given numeric training data. A natural link exists between Petri nets and Probabilistic Logic Programming [26]. Transitions sometimes have firing likelihood constraints and the uncertainty can be modelled by probabilistic logic programs. Evaluating these programs requires tensor-based algebra of logic programs, a topic that has been explored recently in [65].

$BMLP_{active}$ also requires a pre-defined hypothesis space since it does not invent predicates for learning new concepts. This relates to a central problem of ILP known as predicate invention [23]. New predicate names and reusable definitions automatically learned in addition to the background knowledge are machine inventions. Recent methods have combined ILP with meta-level logic programs and matrices such as the Deeplog system [51], δ ILP [29] and *Meta_Abd* [24]. Reusing invented predicates can reduce the size of a hypothesis learned by an ILP system and improve its learning performance [23]. $BMLP_{active}$ could be extended with predicate invention for learning novel biological knowledge.

To make a biological discovery, we aim to integrate this approach with an experiment workflow such as the one shown in [78] to address whole-genome function learning. Data created from a high-throughput empirical framework can be first compared with simulated phenotypic predictions. The inconsistency can inform us of the error sources in the biological model, narrowing the scope of hypothesis space. With advanced biological gene editing tools, genes edition can be targeted for experimental confirmation of candidate hypotheses during active learning. Importantly, we show that our approach can address the interactions between multiple genes, which are not addressable by current mutagenesis approaches.

Designing experiments to explain some hypothesised phenomenon requires deliberate thinking by scientists. A helpful scientific assistant could teach scientists to create experiment plans with optimal outcomes. This aspect of human-AI collaboration has been studied in an emerging research area on Ultra-Strong Machine Learning (USML) [46]. A USML not only learns a concept but also teaches this concept to humans such that human comprehension is improved. Prior research has shown instances of USML in the context of learning recursive concepts [53] and a two-player game [2]. A recent study [1] demonstrated that an ILP system can play the role of a “teacher” and human learning from machine explanations of its output can sometimes inspire human discovery. To date, there is no demonstration of autonomous discovery systems that satisfy the USML criterion. The ultimate goal of autonomous discovery systems is to acquire new scientific understanding and explain insights to humans [41]. The present work can be extended to examine the effect of machine-selected experiments and machine-learned output on human experiment selection and human comprehension of complex biological concepts.

Ethical Statement

Datasets used do not contain any personal information or other sensitive content. There are no ethical issues.

Data Availability

Data used and generated in all experimental sections are accessible on https://github.com/lai1997/BMLP_active_public.

Acknowledgments

The first, third and fourth authors acknowledge support from the UKRI 21EBTA: EB-AI Consortium for Bioengineered Cells & Systems (AI-4-EB) award (BB/W013770/1). The second author acknowledges support from the UK’s EPSRC Human-Like Computing Network (EP/R022291/1), for which he acts as Principal Investigator. ChatGPT and Grammarly have been used as language editing tools after all intellectual content has been drafted.

References

1. L. Ai, J. Langer, S. H. Muggleton, and U. Schmid. Explanatory machine learning for sequential human teaching. *Machine Learning*, 112:3591–3632, 2023.
2. L. Ai, S. Muggleton, C. Hocquette, M. Gromowski, and U. Schmid. Beneficial and harmful explanatory machine learning. *Machine Learning*, 110:695–721, 2021.
3. C. Angione. Human Systems Biology and Metabolic Modelling: A Review—From Disease Metabolism to Precision Medicine. *BioMed Research International*, 2019:e8304260, 2019.
4. D. Angluin. Queries Revisited. In *Proceedings of the 12th International Conference on Algorithmic Learning Theory*, ALT '01, pages 12–31, Berlin, Heidelberg, 2001. Springer-Verlag.
5. S. Anwar, C. Baral, and K. Inoue. Encoding Higher Level Extensions of Petri Nets in Answer Set Programming. In P. Cabalar and T. C. Son, editors, *Logic Programming and Nonmonotonic Reasoning*, Lecture Notes in Computer Science, pages 116–121, Berlin, Heidelberg, 2013. Springer.
6. G. W. Beadle and E. L. Tatum. Genetic Control of Biochemical Reactions in Neurospora. *Proceedings of the National Academy of Sciences*, 27(11):499–506, 1941.
7. T. M. Behrens and J. Dix. Model checking multi-agent systems with logic based Petri nets. *Annals of Mathematics and Artificial Intelligence*, 51(2):81–121, 2007.
8. C. Berge. *Hypergraphs: combinatorics of finite sets*. North-Holland mathematical library. North Holland Distributors for the U.S.A. and Canada, Elsevier Science Pub. Co, Amsterdam New York, 1989.
9. D. B. Bernstein, B. Akkas, M. N. Price, and A. P. Arkin. Evaluating E. coli genome-scale metabolic model accuracy with high-throughput mutant fitness data. *Molecular Systems Biology*, 19(12), 2023.
10. A. Blumer, A. Ehrenfeucht, D. Haussler, and M. K. Warmuth. Occam’s Razor. *Information Processing Letters*, 24(6):377–380, 1987.
11. D. A. Boiko, R. MacKnight, B. Kline, and G. Gomes. Autonomous chemical research with large language models. *Nature*, 624(7992):570–578, 2023.
12. A. M. Bran, S. Cox, O. Schilter, C. Baldassari, A. White, and P. Schwaller. Augmenting large language models with chemistry tools. In *NeurIPS 2023 AI for Science Workshop*, 2023.
13. S. L. Brunton, J. L. Proctor, and J. N. Kutz. Discovering governing equations from data by sparse identification of nonlinear dynamical systems. *Proceedings of the National Academy of Sciences*, 113(15):3932–3937, 2016.
14. C. H. Bryant, S. H. Muggleton, S. G. Oliver, D. Kell, P. Reiser, and R. D. King. Combining inductive logic programming, active learning and robotics to discover the function of genes. *Electronic Transactions in Artificial Intelligence*, pages 1–36, 2001.
15. S. Ceri, G. Gottlob, and L. Tanca. What you always wanted to know about Datalog (and never dared to ask). *IEEE Transactions on Knowledge and Data Engineering*, 1(1):146–166, 1989.
16. S. Y. Choi, K.-h. Yoon, J. I. Lee, and R. J. Mitchell. Violacein: Properties and Production of a Versatile Bacterial Pigment. *BioMed Research International*, 2015:1–8, 2015.
17. W. Cohen, F. Yang, and K. R. Mazaitis. TensorLog: A Probabilistic Database Implemented Using Deep-Learning Infrastructure. *Journal of Artificial Intelligence Research*, 67:285–325, 2020.
18. D. Cohn, L. Atlas, and R. Ladner. Improving generalization with active learning. *Machine Learning*, 15(2):201–221, 1994.
19. D. Conklin and I. H. Witten. Complexity-based induction. *Machine Learning*, 16(3):203–225, 1994.
20. I. M. Copilowish. Matrix Development of the Calculus of Relations. *The Journal of Symbolic Logic*, 13(4):193–203, 1948.
21. M. Costanzo, E. Kuzmin, J. van Leeuwen, B. Mair, J. Moffat, C. Boone, and B. Andrews. Global Genetic Networks and the Genotype-to-Phenotype Relationship. *Cell*, 177(1):85–100, 2019.
22. M. Costanzo, B. VanderSluis, E. N. Koch, et al. A global genetic interaction network maps a wiring diagram of cellular function. *Science*, 353(6306), 2016.
23. A. Cropper, S. Dumancic, R. Evans, and S. H. Muggleton. Inductive logic programming at 30. *Machine Learning*, 111:147–172, 2021.

24. W.-Z. Dai and S. H. Muggleton. Abductive Knowledge Induction from Raw Data. In Z.-H. Zhou, editor, *Proceedings of the Thirtieth International Joint Conference on Artificial Intelligence, IJCAI-21*, pages 1845–1851. International Joint Conferences on Artificial Intelligence Organization, 2021.
25. S. Dasgupta. Coarse sample complexity bounds for active learning. In *Advances in Neural Information Processing Systems*, volume 18. MIT Press, 2005.
26. L. De Raedt and A. Kimmig. Probabilistic (logic) programming concepts. *Machine Learning*, 100(1):5–47, 2015.
27. Y. Dimopoulos, E. Kouppari, A. Philippou, and K. Psara. Encoding Reversing Petri Nets in Answer Set Programming. In I. Lanese and M. Rawski, editors, *Reversible Computation*, Lecture Notes in Computer Science, pages 264–271, Cham, 2020. Springer International Publishing.
28. A. Domenici. Petri nets in logic. *Microprocessing and Microprogramming*, 30(1):193–198, 1990.
29. R. Evans and E. Grefenstette. Learning Explanatory Rules from Noisy Data. *Journal of Artificial Intelligence Research*, 61:1–64, 2018.
30. L. Faure, B. Mollet, W. Liebermeister, and J.-L. Faulon. A neural-mechanistic hybrid approach improving the predictive power of genome-scale metabolic models. *Nature Communications*, 14(1):4669, 2023.
31. M. J. Fischer and A. R. Meyer. Boolean matrix multiplication and transitive closure. In *12th Annual Symposium on Switching and Automata Theory (SWAT 1971)*, pages 129–131, 1971.
32. M. Gelfond and V. Lifschitz. The Stable Model Semantics for Logic Programming. In *Proceedings of International Logic Programming Conference and Symposium*, pages 1070–1080, 1988.
33. E. Grefenstette. Towards a Formal Distributional Semantics: Simulating Logical Calculi with Tensors. In *Proceedings of the Second Joint Conference on Lexical and Computational Semantics (SEM)*, pages 1–10, 2013.
34. R. Guimerà, I. Reichardt, A. Aguilar-Mogas, F. A. Massucci, M. Miranda, J. Pallarès, and M. Sales-Pardo. A Bayesian machine scientist to aid in the solution of challenging scientific problems. *Science Advances*, 6(5), 2020.
35. D. Heckmann, C. J. Lloyd, N. Mih, Y. Ha, D. C. Zielinski, Z. B. Haiman, A. A. Desouki, M. J. Lercher, and B. O. Palsson. Machine learning applied to enzyme turnover numbers reveals protein structural correlates and improves metabolic models. *Nature Communications*, 9(1):5252, 2018.
36. C. Hocquette and S. Muggleton. How Much Can Experimental Cost Be Reduced in Active Learning of Agent Strategies? In F. Riguzzi, E. Bellodi, and R. Zese, editors, *Inductive Logic Programming*, volume 11105, pages 38–53. Springer International Publishing, Cham, 2018.
37. Y. E. Ioannidis. On the Computation of the Transitive Closure of Relational Operators. In *Proceedings of the 12th International Conference on Very Large Data Bases, VLDB '86*, pages 403–411, San Francisco, CA, USA, 1986.
38. R. D. King, J. Rowland, S. G. Oliver, M. Young, W. Aubrey, E. Byrne, M. Liakata, M. Markham, P. Pir, L. N. Soldatova, A. Sparkes, K. E. Whelan, and A. Clare. The Automation of Science. *Science*, 324(5923):85–89, 2009.
39. R. D. King, K. E. Whelan, F. M. Jones, P. G. K. Reiser, C. H. Bryant, S. H. Muggleton, D. B. Kell, and S. G. Oliver. Functional genomic hypothesis generation and experimentation by a robot scientist. *Nature*, 427:247–252, 2004.
40. Z. A. King, J. Lu, A. Dräger, P. Miller, S. Federowicz, J. A. Lerman, A. Ebrahim, B. O. Palsson, and N. E. Lewis. BiGG Models: A platform for integrating, standardizing and sharing genome-scale models. *Nucleic Acids Research*, 44(D1):D515–D522, 2016.
41. M. Krenn, R. Pollice, S. Y. Guo, and others. On scientific understanding with artificial intelligence. *Nature Reviews Physics*, 4:761–769, 2022.
42. P. W. Langley, H. A. Simon, G. Bradshaw, and J. M. Zytkow. *Scientific Discovery: Computational Explorations of the Creative Process*. The MIT Press, 1987.
43. F. Lin. From Satisfiability to Linear Algebra. Technical report, Hong Kong University of Science and Technology, 2013.
44. J. W. Lloyd. *Foundations of Logic Programming*. Springer Science and Business Media, 2012.
45. K. Martínez-Gómez, N. Flores, H. M. Castañeda, G. Martínez-Batallar, G. Hernández-Chávez, O. T. Ramírez, G. Gosset, S. Encarnación, and F. Bolívar. New insights into

- Escherichia coli metabolism: carbon scavenging, acetate metabolism and carbon recycling responses during growth on glycerol. *Microbial Cell Factories*, 11(1):46, 2012.
46. D. Michie. Machine learning in the next five years. In *Proceedings of the 3rd European Working Session on Learning*, pages 107–122. Pitman, 1988.
 47. T. M. Mitchell. Generalization as search. *Artificial Intelligence*, 18:203–226, 1982.
 48. J. M. Monk, C. J. Lloyd, E. Brunk, N. Mih, A. Sastry, Z. King, R. Takeuchi, W. Nomura, Z. Zhang, H. Mori, A. M. Feist, and B. O. Palsson. iML1515, a knowledgebase that computes escherichia coli traits. *Nature Biotechnology*, 35(10):904–908, 2017.
 49. S. H. Muggleton. Inductive logic programming. *New Generation Computing*, 8:295–318, 1991.
 50. S. H. Muggleton. Inverse entailment and Progol. *New Generation Computing*, 13:245–286, 1995.
 51. S. H. Muggleton. Hypothesizing an algorithm from one example: the role of specificity. *Philosophical Transactions of the Royal Society A: Mathematical, Physical and Engineering Sciences*, 381(2251):20220046, 2023.
 52. S. H. Muggleton and C. H. Bryant. Theory completion using inverse entailment. In *Proceedings of the 10th International Workshop on Inductive Logic Programming (ILP-00)*, pages 130–146, 2000.
 53. S. H. Muggleton, U. Schmid, C. Zeller, A. Tamaddoni-Nezhad, and T. Besold. Ultra-strong machine learning: Comprehensibility of programs learned with ILP. *Machine Learning*, 107:1119–1140, 2018.
 54. S. Nienhuys-Cheng and R. Wolf. *Foundations of Inductive Logic Programming*. Springer-Verlag New York, Inc., 1997.
 55. T. Oyetunde, D. Liu, H. G. Martin, and Y. J. Tang. Machine learning framework for assessment of microbial factory performance. *PLOS ONE*, 14(1):e0210558, 2019.
 56. B. O. Palsson. *Systems Biology: Constraint-based Reconstruction and Analysis*. Cambridge University Press, Cambridge, 2015.
 57. C. S. Peirce. *Collected Papers of Charles Sanders Peirce, Volumes II*. Harvard University Press, 1932.
 58. B. K. Petersen, M. L. Larma, T. N. Mundhenk, C. P. Santiago, S. K. Kim, and J. T. Kim. Deep symbolic regression: Recovering mathematical expressions from data via risk-seeking policy gradients. In *Proceedings of the 9th International Conference on Learning Representations*, 2020.
 59. M. N. Price, G. M. Zane, J. V. Kuehl, R. A. Melnyk, J. D. Wall, A. M. Deutschbauer, and A. P. Arkin. Filling gaps in bacterial amino acid biosynthesis pathways with high-throughput genetics. *PLOS Genetics*, 14(1):e1007147, 2018.
 60. P. Rana, C. Berry, P. Ghosh, and S. S. Fong. Recent advances on constraint-based models by integrating machine learning. *Current Opinion in Biotechnology*, 64:85–91, 2020.
 61. W. Reisig. *Understanding Petri Nets: Modeling Techniques, Analysis Methods, Case Studies*. Springer, Berlin, Heidelberg, 2013.
 62. Z. Ren, Z. Ren, Z. Zhang, T. Buonassisi, and J. Li. Autonomous experiments using active learning and AI. *Nature Reviews Materials*, 8(9):563–564, 2023.
 63. G. Rozenberg and J. Engelfriet. Elementary net systems. In *Reisig, W., Rozenberg, G. (eds) Lectures on Petri Nets I: Basic Models. ACPN 1996. Lecture Notes in Computer Science*, volume 1491. Springer Berlin Heidelberg, 1998.
 64. A. Sahu, M.-A. Blätke, J. J. Szymański, and N. Töpfer. Advances in flux balance analysis by integrating machine learning and mechanism-based models. *Computational and Structural Biotechnology Journal*, 19:4626–4640, 2021.
 65. C. Sakama, K. Inoue, and T. Sato. Logic programming in tensor spaces. *Annals of Mathematics and Artificial Intelligence*, 89(12):1133–1153, 2021.
 66. T. Sato. A linear algebraic approach to datalog evaluation. *Theory and Practice of Logic Programming*, 17(3):244–265, 2017.
 67. T. Sato and K. Inoue. Differentiable learning of matricized DNFs and its application to Boolean networks. *Machine Learning*, 112(8):2821–2843, 2023.
 68. T. Sato, K. Inoue, and C. Sakama. Abducing Relations in Continuous Spaces. In *Proceedings of the Twenty-Seventh International Joint Conference on Artificial Intelligence*, pages 1956–1962, 2018.
 69. T. Sato and R. Kojima. Boolean Network Learning in Vector Spaces for Genome-wide Network Analysis. In *Proceedings of the Eighteenth International Conference on Principles of Knowledge Representation and Reasoning*, pages 560–569, Hanoi, Vietnam, 2021. International Joint Conferences on Artificial Intelligence Organization.

70. P. Sen, S. Lamichhane, V. B. Mathema, A. McGlinchey, A. M. Dickens, S. Khoomrung, and M. Orešič. Deep learning meets metabolomics: a methodological perspective. *Briefings in Bioinformatics*, 22(2):1531–1542, 2021.
71. C. Shannon and W. Weaver. *The Mathematical Theory of Communication*. University of Illinois Press, Urbana, 1963.
72. A. Srinivasan. The ALEPH manual. *Machine Learning at the Computing Laboratory, Oxford University*, 2001.
73. A. Srinivasan and M. Bain. Knowledge-Guided Identification of Petri Net Models of Large Biological Systems. In S. H. Muggleton, A. Tamaddoni-Nezhad, and F. A. Lisi, editors, *Inductive Logic Programming*, Lecture Notes in Computer Science, pages 317–331, 2012.
74. A. Tarski. A lattice-theoretical fixpoint theorem and its applications. *Pacific Journal of Mathematics*, 5(2):85–309, 1955.
75. L. Todorovski and S. Džeroski. Integrating knowledge-driven and data-driven approaches to modeling. *Ecological Modelling*, 194(1):3–13, 2006.
76. C. Tosh and S. Dasgupta. Diameter-Based Active Learning. In *Proceedings of the 34th International Conference on Machine Learning*, pages 3444–3452. PMLR, 2017.
77. M. H. Van Emden and R. A. Kowalski. The Semantics of Predicate Logic as a Programming Language. *Journal of the ACM*, 23(4):733–742, 1976.
78. T. Wang, C. Guan, J. Guo, B. Liu, Y. Wu, Z. Xie, C. Zhang, and X.-H. Xing. Pooled CRISPR interference screening enables genome-scale functional genomics study in bacteria with superior performance. *Nature Communications*, 9(1):2475, 2018.
79. S. G. Wu, Y. Wang, W. Jiang, T. Oyetunde, R. Yao, X. Zhang, K. Shimizu, Y. J. Tang, and F. S. Bao. Rapid Prediction of Bacterial Heterotrophic Fluxomics Using Machine Learning and Constraint Programming. *PLoS Computational Biology*, 12(4), 2016.
80. F. Yang, Z. Yang, and W. W. Cohen. Differentiable learning of logical rules for knowledge base reasoning. In *Proceedings of the 31st International Conference on Neural Information Processing Systems*, NIPS’17, pages 2316–2325, Red Hook, NY, USA, 2017. Curran Associates Inc.
81. J. H. Yang, S. N. Wright, M. Hamblin, D. McCloskey, M. A. Alcantar, L. Schrübbers, A. J. Lopatkin, S. Satish, A. Nili, B. O. Palsson, G. C. Walker, and J. J. Collins. A White-Box Machine Learning Approach for Revealing Antibiotic Mechanisms of Action. *Cell*, 177(6):1649–1661, 2019.
82. M. Zampieri, M. Hörll, F. Hotz, N. F. Müller, and U. Sauer. Regulatory mechanisms underlying coordination of amino acid and glucose catabolism in *Escherichia coli*. *Nature Communications*, 10(1):3354, 2019.

Appendix A. Reagent (optional nutrient substance) costs

Carbon Source	Cost per gram (£/g)
D-Mannitol	0.534
Xylose	0.51
Galactose	0.0936
Pyruvate	0.2776
Ribose	0.993
Oxoglutarate	0.437
Acetate	0.0748
Gluconate	0.0359
Glycerol	0.07
Maltose	0.244
Lactate	0.0546
Sorbitol	0.196
Succinate	0.0825
N-acetyl-glucosamine	2.93
L-Alanine	0.81
Glucose	0.0476

Table 2: The costs of 16 optional carbon sources considered in Experiment 2.

Carbon Source	Cost per gram (£/g)
Indole	0.0428
Phenylalanine	0.0346
Tryptophan	0.0346
Tyrosine	0.0346
Shikimate	8.2
L-Aspartic acid	0.0156

Table 3: The costs of aromatic amino acids considered in Experiment 3.

Appendix B. Gene function learning example distribution in Experiment 2.

Table 4: The distribution of synthetic positive and negative examples for each gene knockout based on simulation of iML1515. Gene identifiers start with the lower-case letter “b” and gene descriptive names are given in parentheses.

Gene Id.	$ E^+ $	$ E^- $
b0720 (gltA)	576	121
b1136 (icd)	576	121
b3729 (glmS)	576	121
The other 210 genes	697	0

In Experiment 2, for the 16 carbon sources, 213 genes have a single-knockout phenotypic effect. Three genes, b0720 (gltA), b1136 (icd) and b3729 (glmS), have both positive and negative examples. We focus on b0720 and b3729 since b0720 and b1136 have the same coverage over the 697 training examples so their functions cannot be distinguished.